

1. Report No. [PU-23-RP-02]	2. Government Accession No N/A	3. Recipient's Catalog No. N/A	
4. Title and Subtitle  Unveiling synergistic effects of Nano-modification and CO <sub>2</sub> curing on the durability of precast elements		5. Report Date December 2025	
		6. Performing Organization Code N/A	
7. Author(s)  Mirian Velay-Lizancos (PI), Associate Professor at the Lyles School of Civil and Construction Engineering, Purdue University, 0000-0002-1539-7923 Jan Olek (Co-PI), Professor at the Lyles School of Civil and Construction Engineering, Purdue University, 0000-0003-0467-9877 Raikhan Tokpatayeva, 0000-0003-3663-5131 Aniya Edwards, PhD Student		8. Performing Organization Report No.  PU-23-RP-02	
9. Performing Organization Name and Address  Purdue University Lyles School of Civil and Construction Engineering 550 W Stadium Ave, West Lafayette, IN 47907		10. Work Unit No.  N/A	
		11. Contract or Grant No.  69A3552348333	
12. Sponsoring Organization Name and Address  Transportation Infrastructure Precast Innovation Center (TRANS-IPIC) University of Illinois Urbana-Champaign. Civil & Environmental Engineering. 205 N Mathews Ave, Urbana, IL 61801		13. Type of Report and Period Covered Final Report September 2023 – December 2025	
		14. Sponsoring Agency Code  N/A	
15. Supplementary Notes  For additional reports and information visit the TRANS-IPIC website <a href="https://trans-ipic.illinois.edu">https://trans-ipic.illinois.edu</a>			
16. Abstract  Many precast companies use heating during the curing process to accelerate early strength development and increase production volume without sacrificing durability, as early removal of the forms or transportation with insufficient strength can lead to macro-cracking or micro-cracking. This project has demonstrated that it is possible to reduce the curing time at high temperatures by half by combining CO <sub>2</sub> curing with the addition of recovered carbon black. Thus, this approach can reduce energy consumption and increase precast production, potentially reducing the cost of precast infrastructure elements. Furthermore, when optimized, CO <sub>2</sub> curing not only reduces the time to achieve the target early strength but also reduces porosity, a critical factor in enhancing durability. Results indicated that the combination of CO <sub>2</sub> curing and nano-additive resulted in a reduction in the calcium hydroxide content, thus potentially reducing the risk of durability issues such as calcium oxychloride formation. Besides, the use of recovered carbon black can significantly reduce the hydrophilicity of the cementitious composites.			
17. Key Words  Durability, Precast Curing, Mortar, Cementitious Composites, Carbon Black, CO <sub>2</sub> Curing, Strength Development, Early-Age Strength, Carbonation, Corrosion		18. Distribution Statement  No restrictions.	
19. Security Classification (of this report)  Unclassified.	20. Security Classification (of this page)  Unclassified.	21. No. of Pages  36	22. Price  N/A

**Disclaimer:**

The contents of this report reflect the views of the authors, who are responsible for the facts and the accuracy of the information presented herein. This document is disseminated in the interest of information exchange. The report is funded, partially or entirely, under 69A3552348333 from the U.S. Department of Transportation's University Transportation Centers Program. The U.S. Government assumes no liability for the contents or use thereof.



## **Transportation Infrastructure Precast Innovation Center (TRANS-IPIC)**

### **University Transportation Center (UTC)**

Unveiling synergistic effects of Nano-modification and CO<sub>2</sub> curing on the durability of  
precast elements  
PU-23-RP-02

FINAL REPORT

**Submitted by:**

**Mirian Velay-Lizancos** (PI), Lyles School of Civil and Construction Engineering, [mvelayli@purdue.edu](mailto:mvelayli@purdue.edu)

**Jan Olek** (Co-PI), Lyles School of Civil and Construction Engineering, [olek@purdue.edu](mailto:olek@purdue.edu)

**Raikhhan Tokpatayeva**, Lyles School of Civil and Construction Engineering, [rtokpata@purdue.edu](mailto:rtokpata@purdue.edu)

**Aniya Edwards**, Lyles School of Civil and Construction Engineering, [edwar242@purdue.edu](mailto:edwar242@purdue.edu)

Department: Civil and Construction Engineering

University: Purdue University

**Collaborators / Partners:**

N/A

**Submitted to:**

TRANS-IPIC UTC

University of Illinois Urbana-Champaign

Urbana, IL

## Executive Summary:

Optimizing the application of new technologies and novel materials in precast concrete elements will play a crucial role in advancing the precast industry toward producing ultra-durable precast elements and extending their service life. CO<sub>2</sub> curing of concrete elements, a process well-suited for precast operations, provides a potential benefit by increasing strength while reducing porosity. Similarly, nanomodification via nano-TiO<sub>2</sub> addition in cementitious composites has shown an ability to reduce porosity and increase the strength. Previous studies showed that the use of nano-TiO<sub>2</sub> addition and CO<sub>2</sub> curing has a synergistic benefit, increasing the CO<sub>2</sub> uptake and further reducing the porosity. However, nano-TiO<sub>2</sub> is expensive to acquire. Understanding the impact of using other less expensive nanomaterials on the effects of CO<sub>2</sub> curing process can be instrumental in optimizing the use of both nanomodification and CO<sub>2</sub> curing to create precast elements with enhanced properties while lowering their cost. This project aims (i) to unveil and understand the synergistic effects of nano-modification with affordable nanomaterials and CO<sub>2</sub> curing on the durability and efficacy of precast elements, and (ii) to optimize the CO<sub>2</sub> curing process to enhance early strength and durability, as its effectiveness depends on the relative humidity and the CO<sub>2</sub> concentration used.

In phase I nanosilica (NS) and recovered carbon black (RCB) were evaluated as potential affordable nanoadditives to enhance early strength, both under CO<sub>2</sub> curing and non-CO<sub>2</sub> curing conditions. Notable differences were found between the composition and mechanical characterization of CO<sub>2</sub>-cured and standard-cured cementitious specimens with and without nano-additives (nano-silica and recovered carbon black) at two different water-to-cement (w/c) ratios. Thermogravimetric analysis shows that CO<sub>2</sub> curing greatly increased the CaCO<sub>3</sub> content in samples compared to standard curing. The incorporation of nanoadditives is shown to increase the CaCO<sub>3</sub> content in higher w/c samples, especially when used with CO<sub>2</sub> curing. Compressive test results showed a strength increase in CO<sub>2</sub>-cured specimens compared to standard-cured specimens. Results indicated that the combination of CO<sub>2</sub> curing and nano-additive use resulted in the highest early compressive strength among all mixtures and curing conditions studied (which is very important for precast production), while reducing the calcium hydroxide content, thus potentially reducing the risk of durability issues such as calcium oxychloride formation.

The combination of nanoparticles addition and 12-hour 50°C CO<sub>2</sub> curing process can provide comparable strength to non-nanomodified concretes with a 24-hour 50°C wet curing; reducing the time of high curing temperatures required to achieve the target early strength. While in phase I both NS and RCB were evaluated as potential nanomaterials, due to its lower price, less explored effects, and promising results from the initial stages of this project, RCB was selected for further investigation, in conjunction with CO<sub>2</sub> curing. It is noteworthy that to be used as an additive, recovered carbon black requires a special dispersion method to avoid agglomeration. Mixing the RCB with a small amount of water using a high-shear mixer-blender significantly reduces agglomeration compared to the dry mix method. It was observed that 20% CO<sub>2</sub> curing (no heating) slightly increases strength compared to the 50 °C curing option, for reference and 1% RCB, suggesting that CO<sub>2</sub> curing can be an alternative to steam curing in terms of accelerating the early strength development required to maximize the rate of production of precast elements. Furthermore, the optimal CO<sub>2</sub> concentration to enhance early strength depends strongly on the relative humidity during exposure. Besides, the effectiveness of RCB and CO<sub>2</sub> curing highly depends on the relative humidity. Still, across all mixes, the highest strengths are achieved with 20% CO<sub>2</sub> and 100% RH, without affecting carbonation depth relative to non-CO<sub>2</sub>-cured samples, potentially serving as a more energy-efficient alternative to heat curing used in the precast industry, with no effects on corrosion. Additionally, the CO<sub>2</sub>-curing method reduces the porosity of both the reference and RCB samples. For non-nanomodified mixes, CO<sub>2</sub> curing reduces the hydrophilicity of the cementitious composite, potentially due to a reduction in surface porosity produced during CO<sub>2</sub> curing. The use of 2% RCB clearly increases the hydrophobicity of the composite, but CO<sub>2</sub> curing does not produce a further increase.

This project has demonstrated that it is possible to reduce the curing time at high temperatures by half by combining CO<sub>2</sub> curing with the addition of recovered carbon black. Thus, this approach can reduce energy consumption and increase precast production, potentially reducing the cost of precast infrastructure elements. Furthermore, when optimized, CO<sub>2</sub> curing not only reduces the time to achieve the target early strength but also reduces porosity, a critical factor in enhancing durability.

## Table of Contents

1. Problem Description .....	6
2. Background .....	6
3. Research Scope and Objectives .....	6
4. Research Description .....	7
5. Project results .....	10
5.1. Characterization of the materials .....	10
5.2. Initial curing procedures and assessment of their effects with and without nanoparticles. .....	11
5.3. Analysis of hydration process, porosity and microstructure .....	14
5.4. Initial results of compressive strength of mortars and concretes .....	17
5.5. Transition from Phase I to Phase II: Nanomaterials selection for further investigation ....	19
5.6. Investigation of the influence of relative humidity and temperature on carbonation, values of accessible porosity, and the resulting strength of the CO <sub>2</sub> -cured material.....	20
5.7. Investigation of the influence of the concentration of CO <sub>2</sub> on the effectiveness of the CO <sub>2</sub> curing process in terms of the degree of carbonation, levels of accessible porosity, and strength.....	22
5.8. Analysis of data and determination of the optimal CO <sub>2</sub> curing conditions for various cementitious systems to achieve early compressive and flexural strength.....	25
5.9. Effects of different CO <sub>2</sub> curing conditions, temperature and humidity on the carbonation depth of mortars .....	27
5.10. Corrosion Testing.....	28
5.11. Effect of nano-additives and CO <sub>2</sub> curing on the wettability of cementitious composites. .....	29
6. Outreach activities related to the project.....	31
7. Conclusions and recommendations.....	34
8. Practical application/impact on transportation infrastructure.....	35
9. References.....	35

## 1. Problem Description

The overall objective of the second phase of this project is to improve the quality of precast elements by (i) determining the optimum conditions for CO<sub>2</sub> curing process with and without nano additives to improve durability-related properties, and (ii) quantifying and understanding the combined effects of nano-additive usage and CO<sub>2</sub> curing on the surface wettability and durability. The determination of the optimum CO<sub>2</sub> curing conditions (humidity and CO<sub>2</sub> concentration) to enhance durability-related properties is key to defining an optimized precast CO<sub>2</sub> curing process to enhance durability. Considering preliminary data from phase I on the unchanged pH during CO<sub>2</sub> curing and the reduction of porosity produced by both the use of nano-additives and CO<sub>2</sub> curing, in phase II, the potential reduction of corrosion risk due to CO<sub>2</sub> curing of nano-modified concrete will be assessed. Over the subsequent phases, the general aims of this project will be to: (i) assess the effect of these combined approaches on freeze-thaw resistance and water penetration; (ii) in collaboration with a precast plant, study and test the adaptation of their current curing beds/rooms to include the CO<sub>2</sub> injection process and test different methods of nanomaterials dispersion to determine the best application method in a precast plants' settings; (iii) compare the lab results with precast plant results and understand potential opportunities and challenges to provide guidance for the implementation of these combined approaches and conduct economical and life cycle assessments of different approaches and their combination for comparative evaluation of the effects of applying CO<sub>2</sub> curing for precast elements with nanomodified concrete vs plain concretes.

## 2. Background:

CO<sub>2</sub> curing of concrete elements, a process well-suited for precast operations, was reported to produce an increase in strength and reduce the porosity of the element in two main ways: (i) directly through carbonation during the CO<sub>2</sub> curing process, and (ii) by reducing the amount of cement required to achieve a target performance due to the enhancement of strength [1]. Furthermore, during carbonation, the Calcium Hydroxide (CH) reacts with the CO<sub>2</sub> forming Calcium Carbonate. The reduction of CH resulting from carbonation can increase the durability of concrete, since CH is a harmful component in many durability issues (sulfate attack [2–4], Calcium oxychloride formation [5–7], Alkali-Silica Reaction [7,8], CH leaching [9]). However, CH reduction can affect the ability of concrete to protect steel reinforcement from corrosion due to the reduction of pH of concrete. Thus, the reduction of CH content can be especially beneficial for the durability of non-steel reinforced precast elements, such as concrete blocks and concrete pavers, among others.

On the other hand, nano-TiO<sub>2</sub> addition in cementitious composites has also shown their ability to reduce porosity and increase the strength [10,11]. Furthermore, our previous studies showed that the combination of both nano-TiO<sub>2</sub> addition and CO<sub>2</sub> curing can increase the CO<sub>2</sub> uptake and further reduce the porosity [11]. However, nano-TiO<sub>2</sub> is more expensive than other nanomaterials such as Nano-silica or Nano-carbon black. The effects of different nanoparticle additions on the hydration and morphology of hydration products may modify the impact of CO<sub>2</sub> curing process on the precast elements. Understanding the impact of using different nanomaterials on the effects of CO<sub>2</sub> curing process can be instrumental with respect to optimizing the combined use of nanomodification and CO<sub>2</sub> curing to produce superior precast elements while lowering their cost by making the process more effective and preventing unexpected side effects.

## 3. Research Scope and Objectives:

*Year 1:* This project aims to unveil and understand the synergistic effects of Nano-modification and CO<sub>2</sub> curing on the durability of precast elements. The first phase of this project aimed to elucidate the combined effects of CO<sub>2</sub> curing and nanomodification with alternative nano-additives concerning strength of precast cementitious composites, porosity, and transport properties of precast cementitious composites; properties that are key to the durability of precast transportation infrastructure.

Year 2: The overall objective of the second phase of this project [2<sup>nd</sup> year] is to improve the quality of precast elements by (i) determining the optimum conditions for CO<sub>2</sub> curing process with and without nano additives to improve durability-related properties and (ii) quantifying and understanding the combined effects of nano-additive usage and CO<sub>2</sub> curing on the surface wettability and durability. The determination of the optimum CO<sub>2</sub> curing conditions (humidity and CO<sub>2</sub> concentration) to enhance durability-related properties is key to defining an optimized precast CO<sub>2</sub> curing process to improve durability. Considering preliminary data from phase I on the unchanged pH during CO<sub>2</sub> curing and the reduction of porosity produced by both the use of nano-additives and CO<sub>2</sub> curing, in phase II, the potential reduction of corrosion risk due to CO<sub>2</sub> curing of nano-modified concrete will be assessed.

#### 4. Research Description:

Phase I:

**Task 1. Characterization of the materials.** This task will involve the physical and chemical characterization of the nanoparticles, the aggregates, and the cement to be used in this study, according to the relevant standards for each type of the proposed material. Particle size, oxide and mineralogical content analyses will be performed.

**Task 2. Preparation of specimens and curing process.** Concrete, mortar and cement paste mixtures with 0%, 0.5%, 1%, and 2% of nanoparticles by mass of cement and two different water-to-cement ratios will be used in this study. Two different nanomaterials will be used: nano-silica and carbon black. Thus, a total of 14 different mixtures will be studied for each cementitious composite (paste, mortar and concrete). Specimens will be used to perform microstructural analysis, chemical analysis, and to determine the compressive strength development, transport properties and durability performance. Two different curing conditions and times will be examined: (i) standard curing at  $21 \pm 1$  °C and  $50\% \pm 5\%$  RH (for reference), (ii) CO<sub>2</sub> curing (20% concentration) for 12 hours (from age 24h to 36h) at a temperature of  $23 \pm 1$  °C and  $50\% \pm 5\%$  RH.

**Task 3. Analysis of hydration process, porosity and microstructure.** Microscopic Image analysis of the polished section of concrete will be used as a direct quantification of pore volume, whereas water absorption and density tests will be applied for evaluation of other parameters of the pore structure (ASTM C642<sup>12</sup>, ASTM C1585<sup>13</sup>). Besides, the microstructure of samples will be investigated through Scanning Electron Microscopy (SEM). The hydration kinetics and hydration products of the pastes will be estimated by Isothermal Calorimeter test (IC), Thermogravimetric (TGA) and X-ray diffraction (XRD) analyses.

**Tasks 4. Evaluation of transport properties.** The bulk electrical resistivity and formation factor of the concrete samples will be estimated as per ASTM 1876-19<sup>14</sup>. The Rapid Chloride permeability test (ASTM C1202<sup>15</sup>) will be used to evaluate the resistance of the concretes to chloride ions ingress. The transport properties will be assessed through the analysis of the results of this section in combination with the results from water absorption test performed in task 3. Due to results from other tasks, and changes in the curing procedures based on the initial results, this task was substituted by an extended task 5 with different curing procedures, as well as direct measurements of corrosion. As a result of the extra testing and outreach activities that were not initially planned but were required later, the testing of task 4 was initially delayed and later modified to focus more on direct durability measurements through corrosion testing in phase II.

**Tasks 5. Compressive strength of mortars and concretes.** Compressive strength tests will be performed for each mixture design at 3, 7, and 28 days according to ASTM C39<sup>16</sup>. This task was modified by testing samples with varying curing conditions.

**Task 6. Analysis of the results.** A comparative analysis of the test results from tasks 1 to 5 for samples with and without nanoparticles and with and without CO<sub>2</sub> curing will be carried out. Then, the interconnection of the results of the different tests will be analyzed to acquire a deeper

understanding on the combined effect of nanoparticle addition and CO<sub>2</sub> curing; This task will help understanding the synergistic effects of CO<sub>2</sub> curing and nanomodification on the concrete's properties, providing insights into the optimal combination.

**Task 7. Draft of the report, Review and submission of Final report.** This task will consist of the preparation, revision and submission of the final report of the project, summarizing the research findings, methodologies, conclusions and recommendations.

## Phase II:

**Task 1. Mixture selection and Trial batches for Phase II study.** Based on the results of Phase I, the research team will select the nano-additives and mixture design parameters for concrete mixtures to be used in Phase II. This task also entails the preparation of the trial batches to validate the efficacy of the selected mixtures

**Task 2. Investigation of the influence of relative humidity and temperature on the levels of carbonation, values of accessible porosity, and the resulting strength of the CO<sub>2</sub>-cured material.** Selected mixtures will include, at minimum, a standard mixture with no nano-additives and two mixtures containing nano-additives. For each mixture, there will be three groups of samples cured for 24 hours at different levels of relative humidity (RH) and temperature and a constant CO<sub>2</sub> concentration. Then, all samples will be cured in a standard curing room with 95%±5% RH, and 21°C±2°C. At age 3 days, for each type of mixture and group, the accessible porosity as well as the flexural and compressive strength, and the thickness of the layer of material affected by a substantial drop in pH value will be determined.

**Task 3. Investigation of the influence of the concentration of CO<sub>2</sub> on the effectiveness of the CO<sub>2</sub> curing process in terms of the degree of carbonation, levels of accessible porosity, and strength.** The mixtures used in this task will be the same as those used in Task 2. For each mixture, there will be three groups of samples cured for 24 hours at three different CO<sub>2</sub> concentrations and at constant RH and temperature based on the results of Task 2. At 3 days, the accessible porosity, the flexural and compressive strength, and the thickness of the carbonated layer with low pH will be determined for each type of mixture within each group.

**Task 4. Analysis of data and determination of the optimal CO<sub>2</sub> curing conditions for various cementitious systems.** In this task, the research team will analyze and crosslink data from tasks 2 and 3. The need for further testing to elucidate potential variations between nanomodified and reference cementitious systems will be determined. If needed, additional testing will be conducted, and the results will be analyzed, facilitating a comprehensive understanding of their performance under different curing conditions.

**Task 5. Casting and preparation of corrosion test samples.** As per the original proposal, three concrete mixtures were planned: one without nano-additives and two with nano-additives. Four beams measuring 11 × 6 × 4.5 in. were to be cast, each reinforced with three #5 rebars. One rebar, positioned near the top of the beam, was to serve as the anode, while the other two acted as cathodes. The beams would be divided into two curing regimes: standard curing and CO<sub>2</sub> curing, the latter using the optimized process identified in previous tasks. Mix designs for corrosion test specimens have been established. However, ASTM G109<sup>17</sup> requires specimens too large for the available CO<sub>2</sub>-curing equipment. To overcome this limitation, we adopted an accelerated corrosion test using “lollipop” mortar specimens inspired by corrosion experiments conducted by Ariyachandrea et. al<sup>18</sup> and Mishra et. al<sup>19</sup>. For each mix type, six 2 × 4 in. mortar cylinders will be cast, each embedded with a single #4 rebar (Figure 1). The intentionally low concrete cover is expected to shorten the time to corrosion initiation. After casting, the cylinders will be split into two curing groups: the determined optimal CO<sub>2</sub> curing method and standard wet curing. Following curing, specimens will be submerged in a chloride solution to promote corrosion. In this setup, a steel sleeve will act as the counter electrode, the embedded rebar as the working electrode, and a

silver/silver chloride electrode as the reference. Corrosion measurements will include the determination of changes in half-cell potential and performing linear polarization experiments. Corrosion performance will be assessed following ASTM C876<sup>20</sup> and a modified ASTM G109 procedure. Parameters including corrosion current, corrosion potential, and current density will be used to quantify performance differences between CO<sub>2</sub>-cured and nano-modified mixtures.

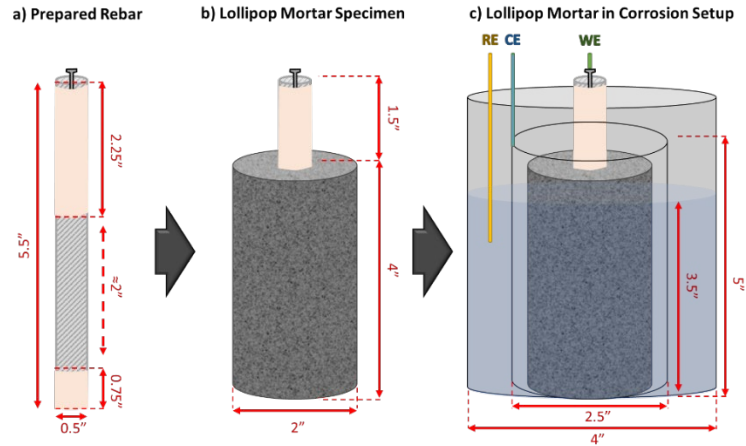


Figure 1. Diagram of Prepared Rebar (a), Reinforced Lollipop Mortar Sample (b), and Corrosion Experiment Setup (c)

**Task 6. Corrosion testing.** The potential for corrosion of reinforcing steel will be evaluated following the general procedure given in ASTM G-109 specification using the samples prepared in Task 5. The primary parameters that will be monitored during this experiment include: macrocell potential, half-cell potential, the corrosion current and depth of chloride penetration. The process of the specimens will be accelerated by exposing submerging samples in chloride solution.

**Task 7. Determination of the effect of nano-additives and CO<sub>2</sub> curing on the wettability of cementitious composites and on the rate of water absorption.** The wettability test will be performed on the surfaces of CO<sub>2</sub>-cured and standard-cured cementitious composites with and without nano-additives.

**Task 8. Outreach activities related to the project.** The preparation and diffusion of short videos and presentations for different audiences (middle school, high school, and university student level) on the following: (i) the importance of sustainable and durable construction practices in transportation and the role of precast concrete elements in the transportation sector (ii) video-tutorials of some tests used in the project for training & workforce development. These videos will be used in addition to the video series in year one of this project to foster interest in engineering and construction research and make engineering practices easily accessible. Annual events will be held in at least one high school of an underserved community for youths interested in civil engineering, construction, and materials science. An activity will be organized for university students interested in research with a hands-on interactive approach. A presentation will be organized for at least one event for industry professionals interested in the use of CO<sub>2</sub> curing, nanomaterials, and sustainable building practices.

**Task 9. Preparation of quarterly reports, draft final report and review.** This task will involve the preparation of quarterly progress reports as well as drafting the final report summarizing the research effort.

## 5. Project results:

### 5.1. Characterization of the materials

Characterization of Nanomaterials: Four nanomaterials, two variants of nanosilica solution (NS) and two variants of carbon black, were evaluated for this project. The carbon blacks evaluated in this project were a standard carbon black (CB) powder, and a recovered carbon black (rCB) acquired from recycled materials. The nanosilica solutions evaluated in this project were a solution with two different nanosilica concentrations. The purity of the carbon blacks was evaluated via loss of ignition (LOI) testing. 0.5 grams of rCB and CB were heated to 900 °C for 3 hours. The LOI tests revealed that the CB was purer than the rCB, burning off 100% of its initial mass compared to 71.83%, respectively (Fig. 2).

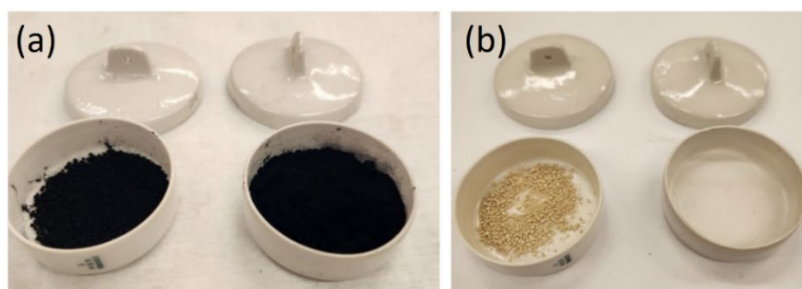


Figure 2. (a) Pre-LOI rCB (Left) and Pure CB (Right); (b) Post-LOI rCB (Left) and Pure CB (Right)

X-ray fluorescence (XRF) analysis and x-ray diffraction (XRD) analysis were used to analyze the mineralogy of both NS, CB, and rCB materials. Both analyses supported that the rCB was less pure than that of the CB, containing a higher presence of zinc and sulfur contaminants. Both followed similar intensity curves to N774 carbon blacks. For nanosilica, these analyses showed that the NS with the highest NS concentration analyzed has approximately 53% concentration of nanosilica compared to a NS of 35% in the lowest concentration NS analyzed. These values are in accordance with the range of concentration levels reported by the NS manufacturer.

Particle size analysis was carried out with laser diffraction and image analysis of transmission electron microscopy (TEM) images. Results from TEM analysis show that the higher concentration NS had particle diameters ranging from 10nm to 90nm (Fig. 3.a), and the rCB has particle sizes ranging from 5nm to 100nm (Fig. 3.b).

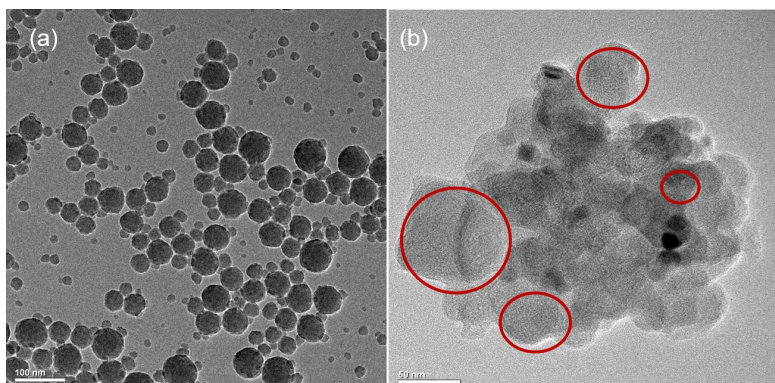


Figure 3. TEM images (a) nanosilica, (b) recovered carbon black.

Based on these analyses, the highly concentrated NS and the less pure rCB were chosen for the mix designs in this project. In the case of carbon black, the decision was made also based on an important difference in the price between pure carbon black and recovered carbon black.

**Characterization of Aggregates:** ASTM C136<sup>21</sup> and AASHTO T27<sup>22</sup> were used to analyze the gradation of fine and coarse aggregates, which was determined to be size 23 fine aggregate and no. 8 coarse aggregate. ASTM C127<sup>23</sup> and ASTM C128<sup>24</sup> were used to evaluate the density and absorption of fine and coarse aggregates, respectively. The absorption of fine and coarse aggregates was verified to be 1.54% and 1.39% respectively. The relative density of fine and coarse aggregates was verified to be 2.65 and 2.75. XRD was also used to analyze the mineralogy of aggregates. Coarse aggregates were made of dolomite while fine aggregates were primarily a mixture of calcite, dolomite, and quartz.

**Characterization of Cement:** XRD and XRF were performed on Type 1L Cement to verify its mineralogy and oxide content. Results revealed that its largest components are alite, belite, and calcite, as expected.

*Table 1: X-Ray Diffraction Results for Type 1L Cement*

Mineral	Type 1L Cement
	Phases (% weight)
Alite	59.88
Belite	13.03
Aluminate	4.05
Ferrite	5.77
Calcite	8.09
Arkanite	0.27
Gypsum	0.29
Anhydrite	0
Bassanite	1.71
Periclase	1.69
Dolomite	2.96
Portlandite	1.04

## 5.2. Initial curing procedures and assessment of their effects with and without nanoparticles.

**Sample size:** Paste and mortar samples were mixed per ASTM C305<sup>25</sup> in batches of eight, 1.25-inch diameter by 0.75-inch samples, and in batches of twenty, 2-inch cube samples (Fig. 4), respectively. Concretes samples were mixed per ASTM C192<sup>26</sup> in batches of thirty-two, 4-inch by 8-inch cylinder samples.



*Figure 4. From left to right; reference, rCB1, and rCB2 mortar samples*

**Dispersion of Nanomaterial:** The NS used has already been dispersed in a liquid form. However, because rCB is a hydrophobic powder material, further dispersion methods were evaluated. The first method consisted of mixing the rCB with the cement powder before following ASTM C305 (Fig. 5a), while the second method involved high shear mixing the rCB with a portion of the batch water using a hand-held blender (Fig. 6a). Samples produced using the first method contained larger agglomerations of rCB in their cross-sections (Fig. 5b) compared to those using the second method (Fig. 6b). The high shear mixing method was therefore adopted for all mixes containing rCB.

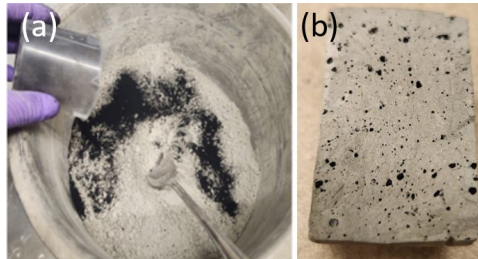


Figure 5. (a) Dry Mix Method: rCB added to cement powder; (b) paste sample made from it

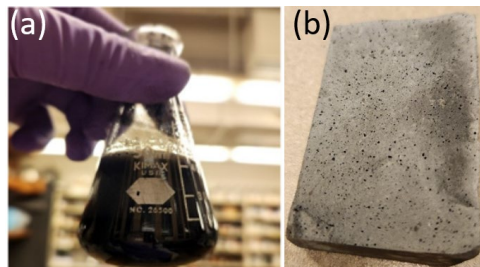


Figure 6. (a) High-Shear Mix Method: rCB blended with water; (b) paste sample made from it

**Curing Procedure of Specimens:** Mortar and paste samples were initially cured under a tarp in the molds for 12 hours. Samples were then transported to an environmental chamber at 50%RH and left to cure for an additional 12 hours. Next, half of the samples were placed in a VWR Symphony CO<sub>2</sub> curing chamber at 23°C with an RH of 95%±5% and CO<sub>2</sub> concentration of 20% for 12 hrs. The other half of samples were placed in a wet chamber with an RH of 95%±5% for 12 hrs. After this 12-hour period, all samples were placed in the wet chamber to cure until their corresponding tests. However, this method saturates the pores of the specimens, which is suspected to reduce CO<sub>2</sub> penetration.

A revised method was instead used for all mortar and paste samples to be analyzed. Mortar and paste samples were in-mold cured and precured in the same conditions. However, following that, half of the samples were placed in a VWR Symphony CO<sub>2</sub> curing chamber at 60°C with an RH ranging from 60%-90% and CO<sub>2</sub> concentration of 20% for 12 hrs. This CO<sub>2</sub> curing method is abbreviated as C. The other half of samples were placed in the environmental chamber with an RH of 50%±5% for 12 hrs. This method is referred to as alternative curing, and is abbreviated with the letter A. After this 12-hour period, all samples were cured in open-air at room temperature and approximately 40%RH after the comparison stage until their corresponding tests. A diagram of this process is shown in Figure 7, and it is the one used for the results summarized in this report. Note that the curing process is the same for both alternative curing and CO<sub>2</sub> curing except during the 12 hours of curing (from age 24 hours to age 36 hours), to be able to assess the effect of the 12-hour CO<sub>2</sub> curing.

## CURING PROCEDURE : PASTES AND MORTARS

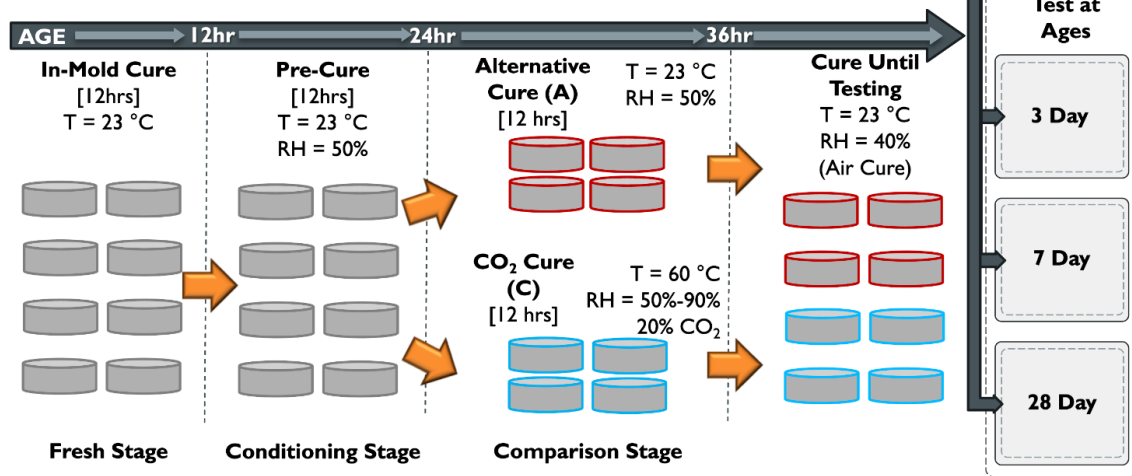


Figure 7. Curing Procedure for Pastes and Mortars

The curing procedure for concretes was adjusted to assess if a short CO<sub>2</sub> curing at 50°C (12 hours) followed by air curing can be a substitute for a longer period (24 hours) of 50°C wet curing process (emulating steam curing). After mixing and casting, the concrete samples were cured in covered plastic molds for 12 hours. Half of the samples were then transported to an environmental chamber at 50%RH and left to cure for an additional 24 hours, while the other half was submerged in a container of water at 50°C to imitate steam curing for 12 hours. This steam curing method is abbreviated as S. Following this 12-hour period, the samples were placed into a TR-HTX CO<sub>2</sub> chamber at 50°C with an RH ranging from 70%±5% and CO<sub>2</sub> concentration of 20% for 12 hrs. At 36 hours of age, all samples were cured in open-air at room temperature and approximately 40%RH after the comparison stage until their corresponding tests. A diagram of this is shown in Figure 8.

## CURING PROCEDURE : CONCRETE

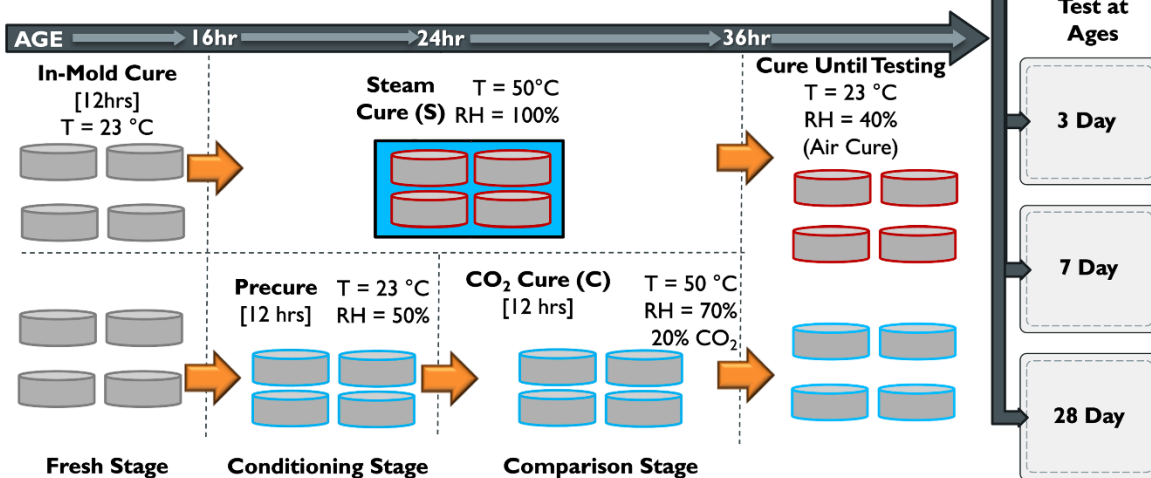


Figure 8. Curing Procedure for Concrete

Naming Conventions: The naming conventions of samples are organized by nanomaterial-percent concentration-(w/c)-curing condition. For example, R(0.42)C refers to a reference mixture with no nanomaterials at a 0.42 w/c that was CO<sub>2</sub> cured. NS1(0.48)A refers to a sample with 1% Nanosilica concentration at 0.48 w/c that was alternatively cured.

### 5.3. Analysis of hydration process, porosity and microstructure

Methods: Image analysis of microstructure of concrete, captured via optical microscope, was used to directly quantify the characteristics of observable porosity. At the same time, water absorption and density tests will be used to evaluate volume of porosity and the connectivity of the pores (ASTM C642<sup>27</sup>, ASTM C1585<sup>28</sup>). Besides, the microstructure of samples was investigated through Scanning Electron Microscopy (SEM). The hydration kinetics and type of hydration products present in the pastes were evaluated by Isothermal Calorimeter test (IC), Thermogravimetric analysis (TGA) and X-ray diffraction (XRD) analysis.

Summary of main results: Isothermal calorimetry analysis of pastes at 0.42 w/c and 0.48 w/c was conducted for a 7-day initial hydration period. Similarly, isothermal calorimetry analysis of mortars at 0.48 w/c was conducted for a 7-day initial hydration period. Results showed that in paste samples, nanomodification generally increases the main peak of the heat flow. However, in mortars at 0.48 w/c, heat flow peak is reduced with rCB nanomodification. An increase in rCB concentration shortens final setting time, however an increase in NS concentration delays final setting time, varying from reference setting time by no more than 15 minutes.

TGA was performed on 0.42 w/c and 0.48 w/c pastes at 3, 7, and 28 days of hydration. The Kim-Olek method<sup>29</sup> was used to quantify prominent compounds like CaCO<sub>3</sub> and CH. Thermogravimetric analysis showed that CO<sub>2</sub> curing greatly increased the CaCO<sub>3</sub> content in samples compared to standard curing. The incorporation of nano-additives is shown to increase the CaCO<sub>3</sub> content in higher w/c (0.48) samples at 3 days (Fig. 9), especially when used with CO<sub>2</sub> curing, except for samples with high nanosilica content (2%). The increase in CaCO<sub>3</sub> in samples over time is accommodated by a prominent decrease in primary hydration products and CH concentration. This reduction of CH resulting from carbonation can increase the durability of concrete, since CH is a harmful component in many durability issues (sulfate attack, Calcium oxychloride formation, Alkali Silica Reaction, CH leaching<sup>1</sup>). However, CH reduction can affect the ability of concrete to protect steel reinforcement from corrosion due to the reduction of pH of concrete. Thus, reduction of CH content can be especially beneficial for the durability of non-steel reinforced precast elements, such as concrete blocks and concrete pavers, among others.

Additional testing planned for phase II will determine the effects on the corrosion risk of steel reinforced concrete elements. This effect at early ages is not as prominent in samples with low water-to-cement ratio. This can be explained by the fact that the low porosity of low w/c mixtures combined with the reduction of porosity produced by the addition of nanoparticles (filling effect), can lead to a very low porosity that decreases the efficiency of CO<sub>2</sub> curing due to the lack of space for the diffusion of CO<sub>2</sub>. Thus, the results indicate that higher w/c can benefit more for the combined effects of CO<sub>2</sub> curing and the use of nanoparticles.

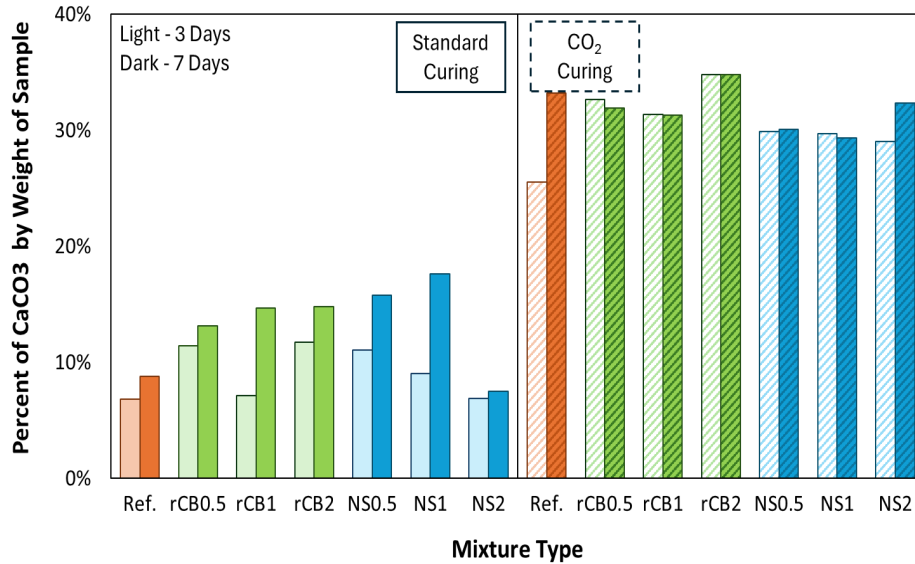


Figure 9. Concentration of CaCO<sub>3</sub> in the surface of 0.48 w/c pastes at 3 and 7 days of hydration

### Scanning Electron Microscopy (SEM) of Pastes

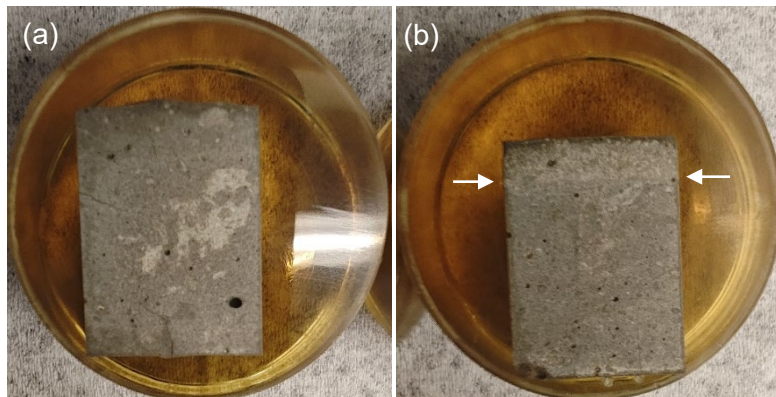
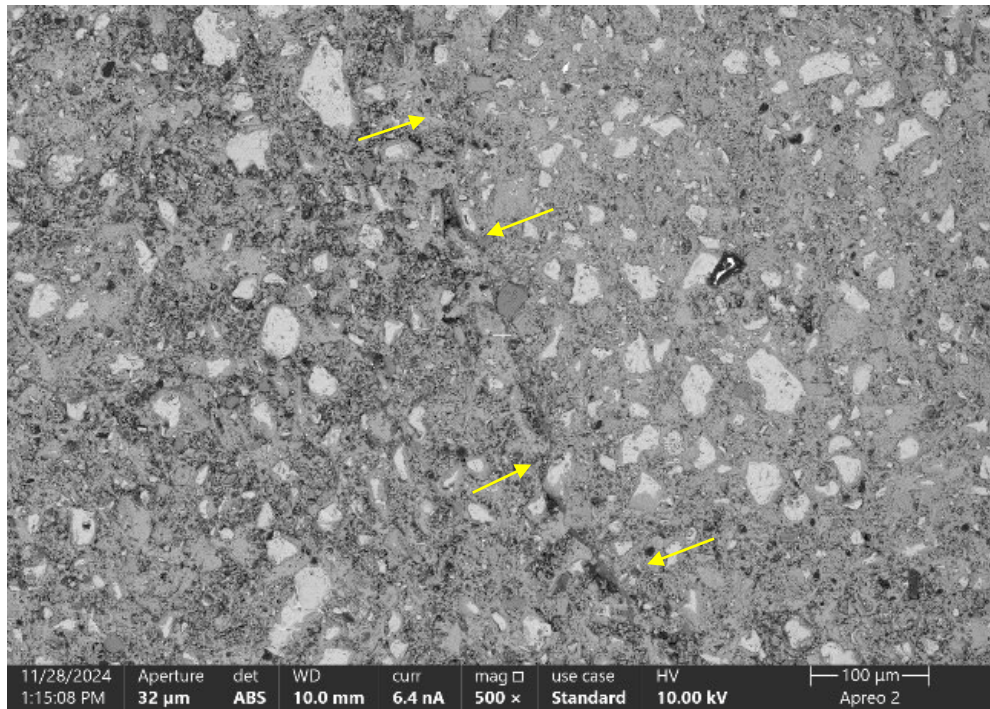


Figure 10. (a) Cross Section of NS2(0.48)A and (b) NS2(0.48)C paste samples

Paste samples at 0.42 w/c and 0.48 w/c 28-day aged samples were epoxy coated and prepped for SEM analysis.

There is a visible difference between the cross-sections of the CO<sub>2</sub> cured and non-CO<sub>2</sub> cured samples. CO<sub>2</sub> cured samples generally have a distinct white layer at approximately 0.2 inches deep, whereas non-CO<sub>2</sub> cured samples have a thinner, fainter layer, if not missing one entirely (Fig. 10). Such transition zones can be seen via SEM, where the white layer transitions from a denser more uniform structure to a more irregular structure (Fig. 11).



*Figure 11. Transition zone of rCB2(0.48)C paste sample. The boundary between the white layer (close to the carbon cured surface) and the rest of the sample is indicated by the yellow arrows.*

Energy dispersive x-ray (EDX) was used to approximate the amount of various chemical elements between different samples. The presence of calcium increases in CO<sub>2</sub> cured specimens when evaluating these transition zones. The more evenly dispersed calcium detections can be seen in Figure 12.

Concrete samples at 0%, 2% rCB, and 2% NS nanomaterial concentrations were mixed and sliced into cylinders corresponding to sizes described in ASTM 1585 and are being conditioned for water absorption, density, and porosity testing. Cement paste samples have been prepared for XRD testing and analysis. The changes in the curing process, based on the results of previous tasks, led to additional testing that was not included in the initial plan. Additionally, while outreach activities were not part of Phase I initially, they were later incorporated. As a result of the extra testing and outreach activities, the completion of the XRD test and analysis is now expected around the end of period for Phase I of the project.

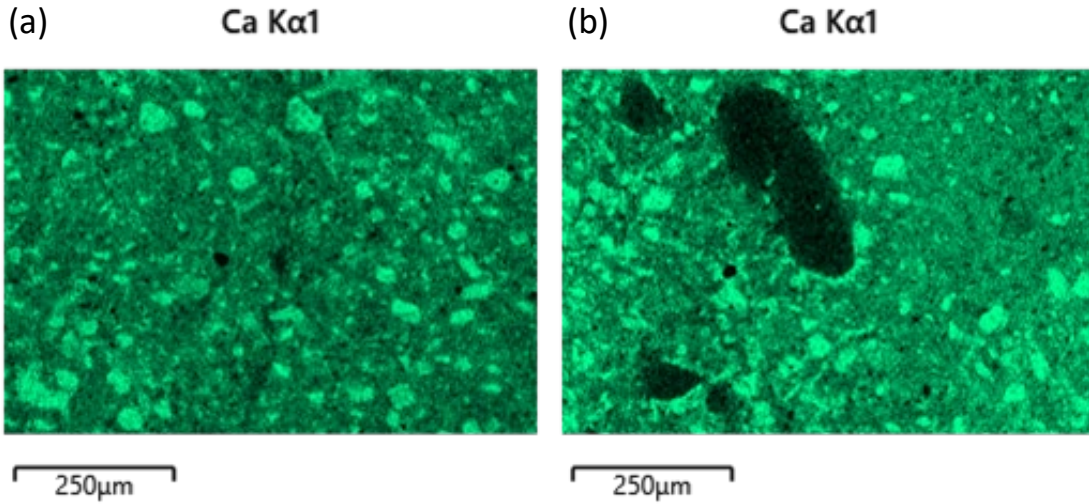


Figure 12. (a) Calcium detection map of rCB2(0.48)A; (b) rCB2(0.48)C at boundary locations, approximately 0.2 inches from sample surface

#### 5.4. Initial results of compressive strength of mortars and concretes

Compression tests over time prove to yield different results on mortars and concretes, due to both their different compositions, and the difference in curing conditions. In mortars, CO<sub>2</sub> curing improves strength for all specimens relative to non-CO<sub>2</sub> cured samples at early ages of 3 (Fig. 13) and 7 days. While nanomodification alone is not showing an increase of early strength, in combination with CO<sub>2</sub> curing shows an increase on early strength compared to non-nanomodified samples under the same CO<sub>2</sub> curing conditions, especially for high contents of rCB and low contents of NS.

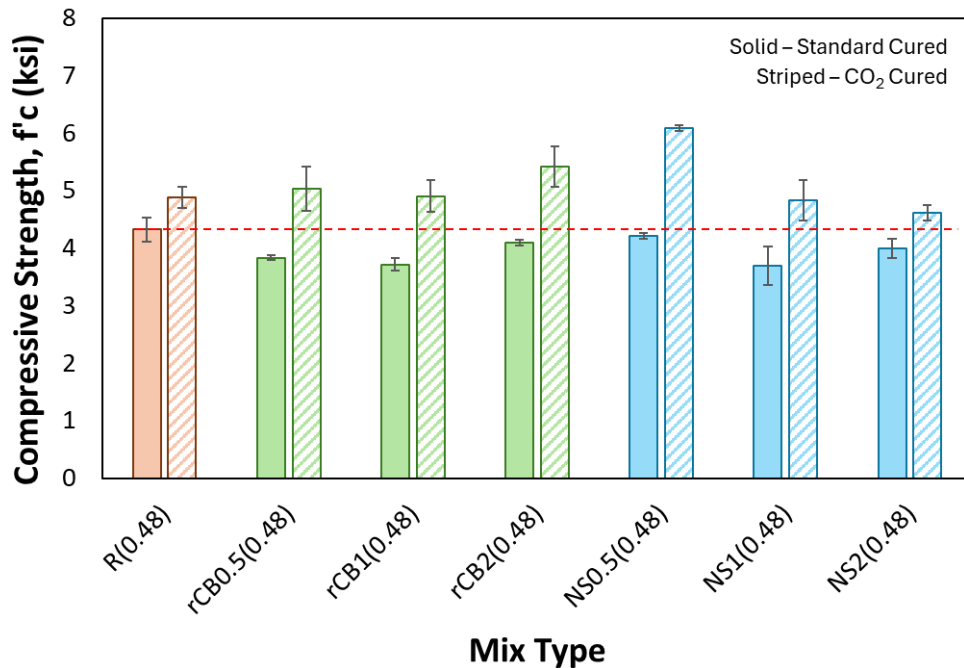


Figure 13. 3-Day f'c of 0.48 w/c Mortars

Figure 14 presents the compressive strength of concrete with two different approaches: (i) with 24 hours of wet at 50°C, compared to (ii) with only 12 hours of CO<sub>2</sub> curing at 50°C; both followed by air curing (Fig. 7), to assess if a short CO<sub>2</sub> curing followed by air curing can be a substitute of a longer period high temperature wet curing process.

It was observed that, while for non-nanomodified samples the CO<sub>2</sub> curing followed by air curing shows slightly lower 7-day strength than water cured samples, when adding nanoparticles and CO<sub>2</sub> curing, we are able to achieve an early strength comparable or even higher than the strength of the reference mixtures (no nanomodified) cured with the 24-hour 50°C wet curing. Thus, the combination of nanoparticles addition and 12-hour 50°C CO<sub>2</sub> curing process can provide comparable strength than non-nanomodified concretes with a 24-hour 50°C wet curing; reducing the time of high curing temperatures required into half.

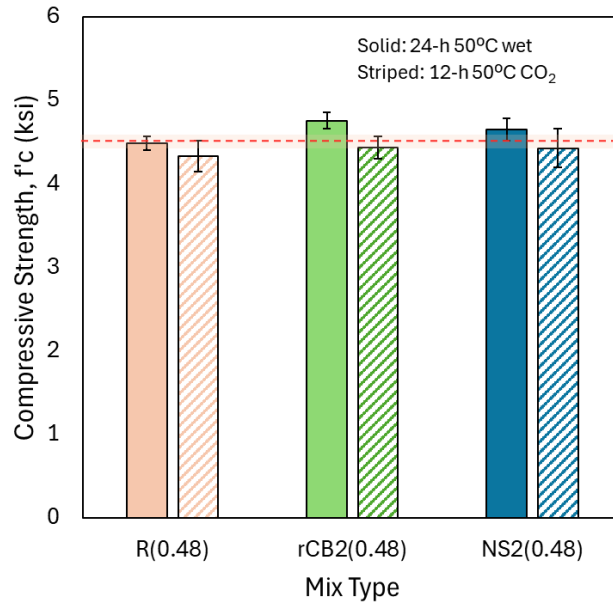


Figure 14. 7-Day  $f'c$  of 0.48 w/c Concretes

Recovered carbon black as a waste valorizing product may prolong the durability of mortars by improving strength through its reuse in precast structures. In combination with CO<sub>2</sub> curing, the use of rCB can provide similar strength to reference concretes with a continuous wet curing process; thus, the combination of CO<sub>2</sub> curing and the use of rCB can reduce the curing time and avoid the need for wet curing for high w/c mixtures, while keeping or increasing the early strength of the precast element.

Reducing curing time, avoiding wet curing, and enhancing the early strength of precast elements can be highly beneficial for the precast industry, increasing the efficiency of its production process. Additional testing to optimize the CO<sub>2</sub> curing process is required, and it is part of Phase II of the project, in order to explore the full potential of this combination and to set the guidelines of the curing process for standard and nanomodified precast elements.

## 5.5. Transition from Phase I to Phase II: Nanomaterials selection for further investigation

Mix designs for the current phase of experimentation were based upon findings from Phase 1 of the project. Phase 1 evaluated the use of both nanosilica (NS) and recovered carbon black (RCB) admixtures at 0%, 0.5%, 1%, and 2% concentration by cement weight in paste, mortar, and concrete. Additionally, to compare the effects of age and water-to-cement ratio (w/c) on the influence of the nanomaterials, two different w/c at 0.42 and 0.48 were used and all composites were evaluated at 3-, 7-, and 28-days of hydration. During this phase, several curing regimens were utilized for effective CO<sub>2</sub> and normal curing of specimens. The findings from that phase of research indicated an increase in strength and calcium carbonate development from the synergistic use of both nanoadditives, however, the extent of this increase was largely based upon the w/c and concentration of nanoadditives used. Additionally, the utilization of both CO<sub>2</sub> curing and nanomodification in concretes cured in a 12-hour 50°C CO<sub>2</sub> curing process provided comparable strength to non-nanomodified concretes with a 24-hour 50°C wet curing process.

Compared to NS, RCB is a more cost-efficient, sustainable additive that benefits from the recycling of waste tires and rubber by products. According to recommendations from the National Precast Concrete Association (NPCA)<sup>30</sup>, w/c less than 0.45 is recommended, and because RCB mixtures performed best at the lower w/c in early-age strength and carbonation development, RCB was selected as the nanomaterial of choice for the current phase of this project. Three types of mixtures were evaluated for this phase: a reference mixture with no nanomaterial (REF), a mixture with 1% RCB addition by weight of cement (RCB1), and a mixture with 2% RCB addition by weight of cement (RCB2). RCB was incorporated into the mixtures using the high shear mixing method explored in Phase 1 of this project; a commercial handheld high shear mixer was used to blend RCB with the batch water for a minimum of 90 seconds, and the blend was added to the cementitious mixture. Mortar and concrete mixtures were composed of Type 1L cement, No. 23 fine aggregate sand, and No.8 coarse aggregate (when needed) and mixed at a w/c of 0.42, meeting NPCA guidelines.

Several discussions with precast concrete manufacturers in the Midwest orchestrated by the graduate student on this project influenced the curing schedule used in this phase. From this correspondence, a 48-hour curing procedure was formulated (Figure 15). After mixing, samples were cured in molds and covered with a tarp for 16 hours at 23°C, retaining moisture to maintain 100% relative humidity (RH). Next, samples were conditioned for 8 hours in a 50% RH chamber at 23°C so that samples can release some of their internal moisture, to allow for effective CO<sub>2</sub> penetration. For the subsequent 24 hours, samples were comparison cured in various RH, CO<sub>2</sub>, and temperature conditions, to thoroughly evaluate the effect of environmental conditions on CO<sub>2</sub> penetration and mechanical performance. These conditions will be compared to normal curing conditions, indicated by no CO<sub>2</sub> exposure, 100% RH, and 23°C. The details of these conditions are thoroughly explored in Tasks 2-4. This completes the experimental curing regimen, and samples were placed in in a 50% RH chamber at 23°C until testing.

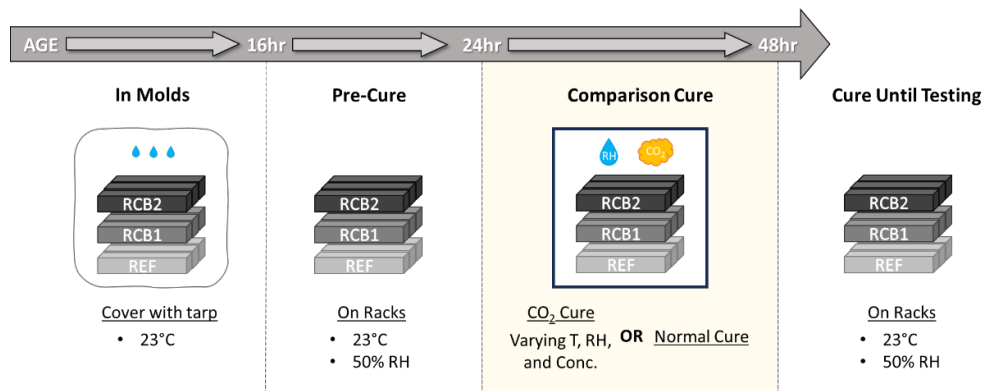


Figure 15. Curing Schedule of Cementitious Composites

**5.6. Investigation of the influence of relative humidity and temperature on carbonation, values of accessible porosity, and the resulting strength of the CO<sub>2</sub>-cured material.**

Three 40mm by 40mm by 160mm mortar prisms were cast for each mix type in Tasks 2-4 (Figure 16). Figure 17 outlines the curing conditions explored during the comparison cure phase for Task 2. For this task, mortar specimens were subject to RHs of 50%, 70%, and 100% RH with no CO<sub>2</sub> exposure. Additionally, 100% RH samples were subject to either 23°C or 50°C (steam curing).



Figure 16. Mortar Prisms After “In-Mold” Process

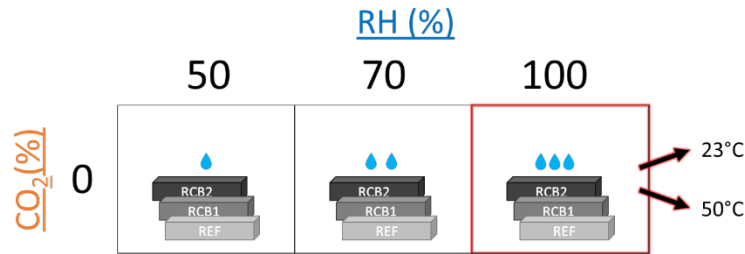


Figure 17. Curing Conditions of Mortar Specimens Cured Without CO<sub>2</sub>

**Flexural Strength:** The flexural strength of mortars was tested at 3 days of hydration (Figure 18) to imitate the early age quality assurance testing done in many precast facilities per ASTM C348<sup>31</sup>. Results show that RCB1 samples have higher flexural strength when cured in lower RH. For instance, among 50% RH samples, RCB1 is 20% stronger in flexure compared to Ref. samples, unlike the 7% reduction displayed by RCB2 samples. While increasing RH has little effect on the strength of Ref. samples, RCB samples decrease in strength as RH increases. Strength reduction of RCB samples in the presence of increased moisture was also seen in Phase 1 of this project, as RCB samples performed better with lower w/c than higher w/c.

Steam cured samples generally have higher strengths than their normal cured counterparts, with reference and RCB2 samples increasing by 35% and 21% when cured in higher temperatures, respectively. This is expected to occur as higher temperatures during curing accelerate the curing rate of cementitious composites.

It is suggested that, due to the hydrophobicity of the RCB additives, micropores are created during mixing, which allow for increased absorption in high moisture conditions, reducing strength. Higher concentrations of RCB are likely to agglomerate during mixing, creating interfacial transitions zones in mortar cross-sections that function as sites prone to cracking.

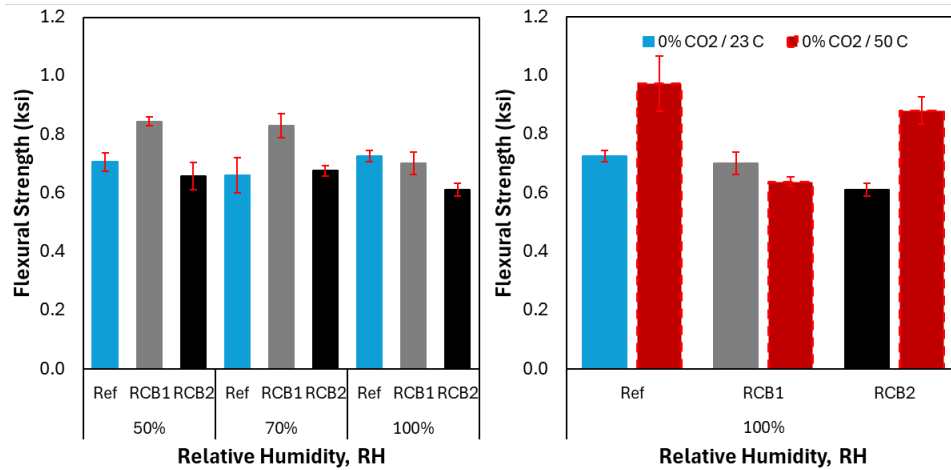


Figure 18. 3- Day Flexural Strength of Mortars Cured in 50%, 70%, 100% RH at 23°C (a) and 50°C (b)

**Compressive Strength:** The compressive strength ( $f'_c$ ) of mortars was also tested at 3 days of hydration (Figure 19) per ASTM C349<sup>32</sup>. Similar to the behavior seen in flexural strength comparisons, RCB1 mortars display highest compressive strengths at low curing RHs, at least 10% higher than Reference samples. However, increasing RH from 50%-100% increases  $f'_c$  of reference mortars by 22%, RCB2 mortars by 9%, and maintains strength in RCB1 mortars.

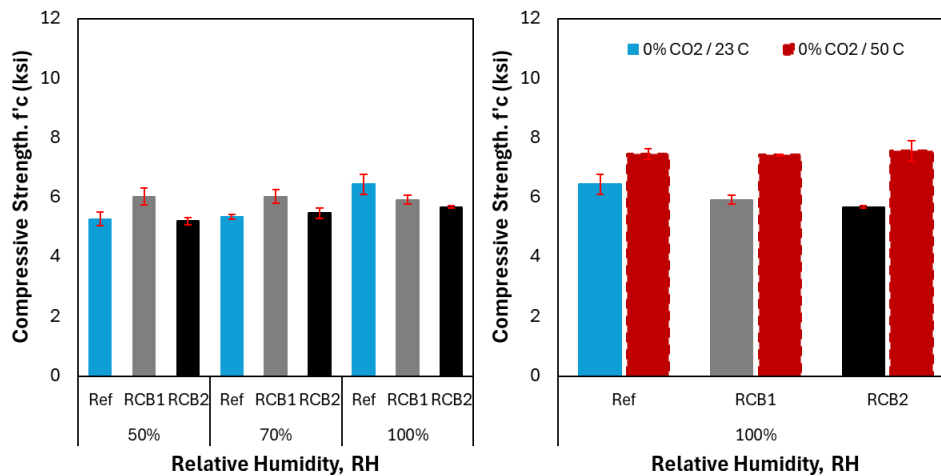


Figure 19. 3-Day  $f'_c$  of Mortars Cured in 50%, 70%, 100% RH at 23°C (a) and 50°C (b)

**Cross-Sectional Change in pH:** After splitting mortars in flexure, their cross-sections were sprayed with aqueous solution of 2% phenolphthalein. Photos were taken of the cross sections after 30 minutes to evaluate the change in cross-sectional pH, where a pink tint on the mortar indicates a pH above 8.3 and a colorless tint indicates a more acidic pH below 8.3. Colorless regions indicate a presence of carbonation, which reduces the pH of cementitious composite.

Figure 20 displays the pH of mortar cured without CO<sub>2</sub> in 50% and 100% RH. There is minimal carbonation penetration in any of the specimens, which is expected to occur without CO<sub>2</sub> treatment. There is also minimal difference between mix groups, as REF, RCB1, and RCB2 have negligible carbonation penetration in their cross-sections. This indicates that strength contributions from nanoadditives, particularly in RCB1 mortars, are not due to carbonation development, and likely due to microstructural or hydration differences in mixes.

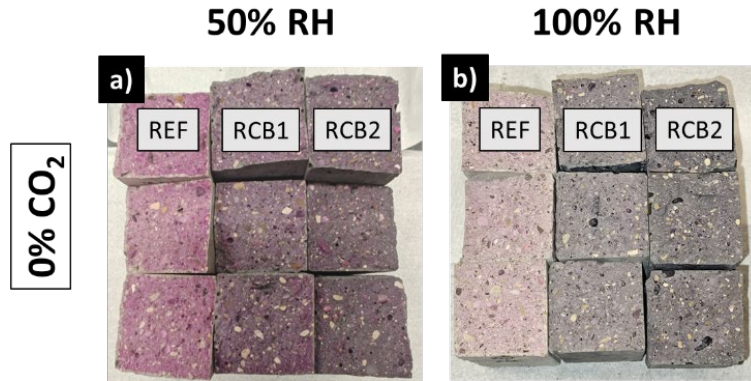


Figure 20. Phenolphthalein Treated Cross-Sections of Mortar Cured in 50%(a) and 100% RH(b) at 23°C

**5.7. Investigation of the influence of the concentration of CO<sub>2</sub> on the effectiveness of the CO<sub>2</sub> curing process in terms of the degree of carbonation, levels of accessible porosity, and strength.**

Figure 21 outlines the curing conditions explored during the Comparison Cure phase for Task 3. For this task, mortar specimens were subject to CO<sub>2</sub> concentrations of 0%, 5%, 10%, and 20% with 100% RH exposure. Lower CO<sub>2</sub> conditions (5-10%) were explored particularly for the potential incorporation of waste flue gas in the CO<sub>2</sub> curing process, which tend to contain between 8-15% of CO<sub>2</sub><sup>33</sup>. Steam cured samples from Task 2 are listed for comparison.

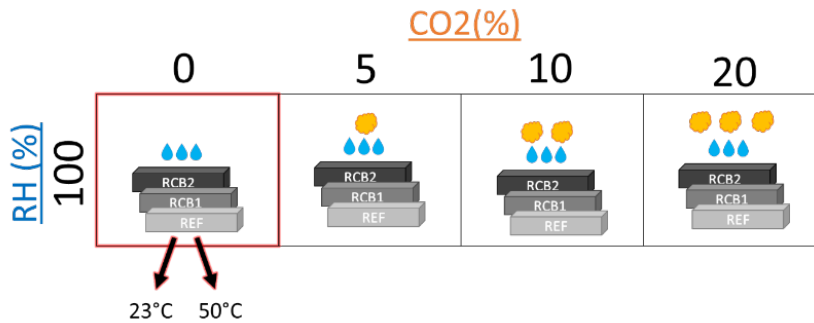


Figure 21. Curing Conditions of Mortar Specimens Cured in 100% RH at varying CO<sub>2</sub> Concentrations

**Flexural Strength:** Results from 3-day flexural strength testing per ASTM C348 are shown in Figure 22. CO<sub>2</sub> curing enhances the flexural strength of all mix types, with 5% CO<sub>2</sub> concentrations during comparison curing respectively increasing REF and RCB1 samples by 21% and 25%. In most circumstances, increasing CO<sub>2</sub> concentration has little effect on or potentially reduces the flexural strength of mortars. This alludes to a potentially beneficial change in the microstructural change of early-age cementitious composites cured in low concentrations of CO<sub>2</sub>. Still, steam-cured reference samples have the highest overall flexural strengths amongst all wet-cured samples.

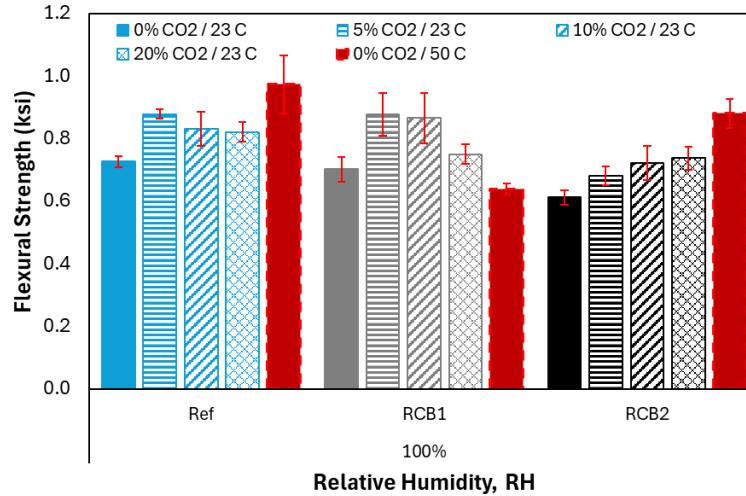


Figure 22. 3- Day Flexural Strength of Mortars Cured in 0%, 5%, 10%, and 20% CO<sub>2</sub> at 23°C and 0% CO<sub>2</sub> at 50°C

**Compressive Strength:** Figure 23 displays compressive strength results per ASTM C349 for mortars cured in 100% RH during the comparison phase. Incorporating RCB into wet-cured mixtures slightly reduces compressive strength with RCB2, when cured at 23 °C, however, for wet-cured at 50 °C, or for CO<sub>2</sub> cured with up to 10% CO<sub>2</sub> at 23 °C, the RCB leads to similar or higher early strength than their corresponding references. As seen in flexural strength patterns, CO<sub>2</sub>-curing can increase the compressive strength of mortar specimens. Yet, 20% CO<sub>2</sub> concentrations result in the highest strength amongst all CO<sub>2</sub> specimens, even matching or exceeding the strength of steam-cured specimens in REF and RCB1 samples by as much as 8%.

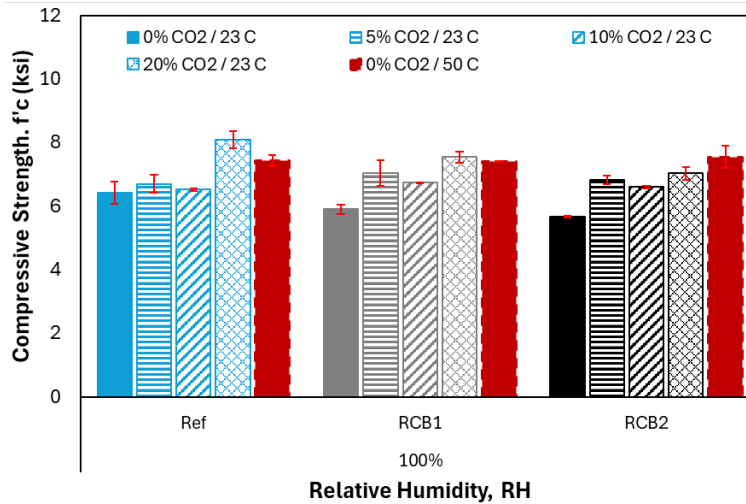


Figure 23. 3-Day f'c of Mortars Cured in 0%, 5%, 10%, and 20% CO<sub>2</sub> at 23°C and 0% CO<sub>2</sub> at 50°C

**Cross-Sectional Change in pH:** Phenolphthalein treatment of mortars cured in varying CO<sub>2</sub> concentrations at 100%RH show minimal carbonation development in all mix types (Figure 24). This supports the concept that high curing humidity could mitigate the effectiveness of CO<sub>2</sub> curing on carbonation development. Yet, this does not support the evidence that CO<sub>2</sub> curing increases the flexural and compressive strength of mortars. For example, exposing RCB1 mortars to 20% CO<sub>2</sub> concentrations increases compressive strength by over 25%, yet no difference is seen in the penetration depth of carbonation during phenolphthalein analysis. This could indicate a different carbonation mechanism

occurring, with the belite being carbonated in high humidity CO<sub>2</sub> treatment, mitigating the reduction of cross sectional pH and thereby not resulting in a color change during testing.

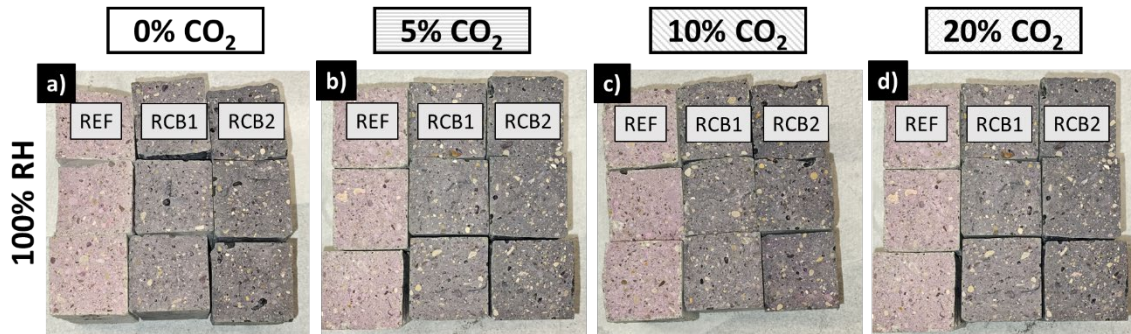


Figure 24. Phenolphthalein Treated Cross-Sections of Mortar Cured in 0%, 5%, 10%, and 20% CO<sub>2</sub> at 23°C

**Absorption, Density, and Porosity:** Porosity measurements were performed on 40mm x 40mm x 160mm prisms according to ASTM C642<sup>34</sup> with the exception that saturation of the specimens was achieved by vacuum instead of boiling the specimens in water, as permitted in Note 2 of the standard. After mixing and casting 6 mortar prisms for each mix group, half were wet cured and the other half cured in 100%RH, 20% CO<sub>2</sub>, 23°C during the comparison curing phase. Subsequent to the curing regimen, all specimens were cured in a 50% RH, 23°C environmental chamber until a 7-day age of hydration where they were weighed and placed into an oven at 110 °C ± 5 °C for 24 hours. Once weighed, they were submerged in water at 23°C and weighed in two, 24-hour increments, ensuring that a constant mass was achieved. Samples were then submerged in a tank filled with water under a vacuum for a minimum of 14 hours, patted dry with a towel to saturated surface dry condition, and weighed thereafter. Finally, the samples were suspended in a tank under water and their buoyant mass was recorded.

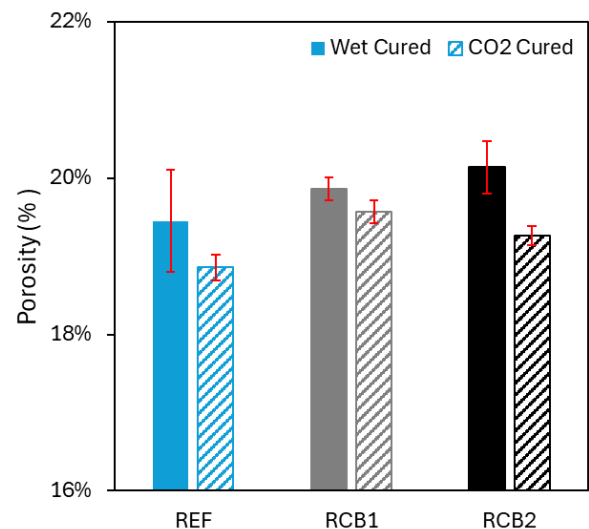


Figure 25. Porosity of CO<sub>2</sub>-Cured and Wet Cured Mortar Prisms

Pore volume calculations indicate a range of 18%-21% for all specimens, as shown in Figure 25. Increasing rCB concentrations is shown to slightly increase mortar porosity, by as much as 5% in rCB2 specimens. This supports the idea that the hydrophobicity of RCB and the repulsion of the mixing water during initial setting could result in increased porosity. However, CO<sub>2</sub> curing reduces porosity than for all mix types, due to the formation of CaCO<sub>3</sub>. This reduction is especially important for samples with rCB2, which can explain the better performance of CO<sub>2</sub> curing when combined with rCB.

Results from testing indicate that increased RCB concentrations slightly increase the absorption of mortar samples by as much as 4% (see Table 2). However, CO<sub>2</sub> curing mortars of all mix types reduces the absorption and increases apparent density, indicating a filling of sample pores due to carbonation. Again, the combination of CO<sub>2</sub> curing and RCB2 yield better results than reference with wet curing, producing samples with lower porosity and water absorption, and higher density.

Table 2: Absorption and Density of CO<sub>2</sub>-Cured and Wet Cured Mortar Prisms

Mix Type		Absorption after Immersion and Vacuum (%)	Apparent Density (g/cm <sup>3</sup> )
REF	Wet Cure	9.5%	2.54
	CO <sub>2</sub> Cure	9.1%	2.57
rCB1	Wet Cure	9.6%	2.57
	CO <sub>2</sub> Cure	9.4%	2.58
rCB2	Wet Cure	9.9%	2.54
	CO <sub>2</sub> Cure	9.4%	2.55

5.8. Analysis of data and determination of the optimal CO<sub>2</sub> curing conditions for various cementitious systems to achieve early compressive and flexural strength

The comparison curing conditions from Tasks 2 and 3 were extended to cover a grid of curing conditions with RHs of 50%, 70%, and 100% and CO<sub>2</sub> concentrations of 0%, 5%, 10%, and 20% (Figure 26). 3D surface plots were created for 3-day flexural strength and f'c of mortars cured under these different regimens, which were tested in the same manner described in Task 2 and 3. This results in 234 samples tested for a collective 39 data points.

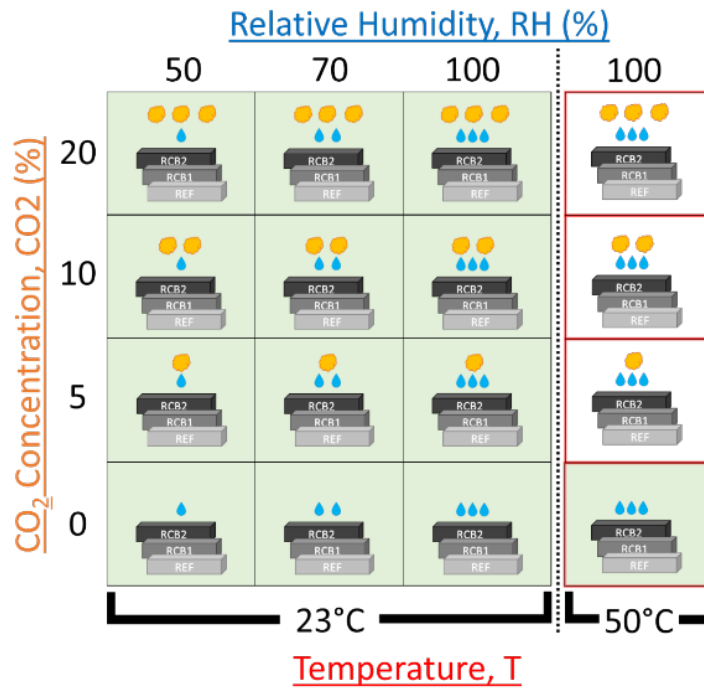


Figure 26. Curing Conditions of Mortars Exposed to Varying CO<sub>2</sub> Concentrations, Relative Humidities, and Temperatures. Conditions evaluated for this project are highlighted in green.

Figure 27 showcases the importance of developing a model that accounts for both CO<sub>2</sub> concentration and relative humidity, and the effectiveness of the CO<sub>2</sub> concentration depends in both the binder and the RH. With a relative humidity of 70%, RCB 1% mixtures perform better than the OPC mixtures (ref) at both normal curing and CO<sub>2</sub> curing up to 10% concentration; the use of 1% RCB combined with 10% CO<sub>2</sub> curing produces an increase of +26% in the 3-day compressive strength when RH is 70% for all

samples (Figure 27.a). However, when the RH is 50%, the increase due to the use of 1% RCB and 10% CO<sub>2</sub> is lower (Figure 27.b).

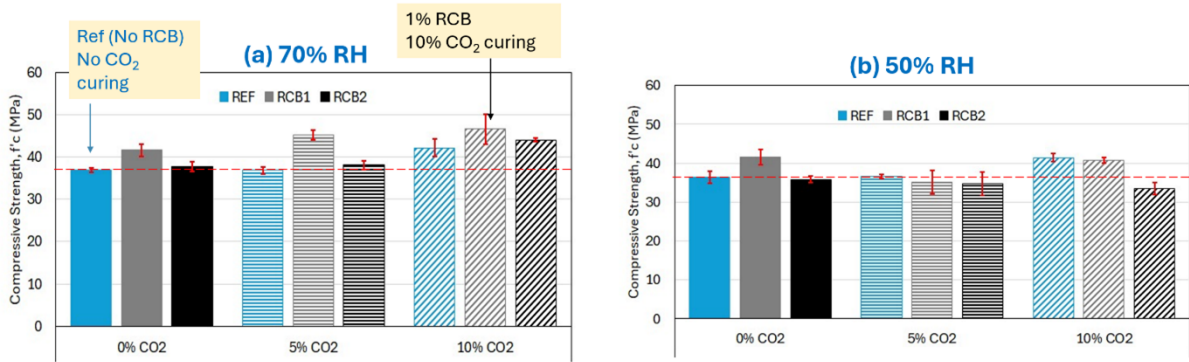


Figure 27. 3-day compressive strength of mortars (a) cured at 70% RH, and (b) cured at 50% RH.

Surface plots from flexural strength testing in Figure 28 reveal that the highest strengths are seen in REF and RCB1 samples cured in 100%RH at low CO<sub>2</sub> concentrations (between 5%-10%). Surface plots also show that a higher CO<sub>2</sub> concentration is potentially more detrimental to early age flexural strength, especially in nanomodified samples.

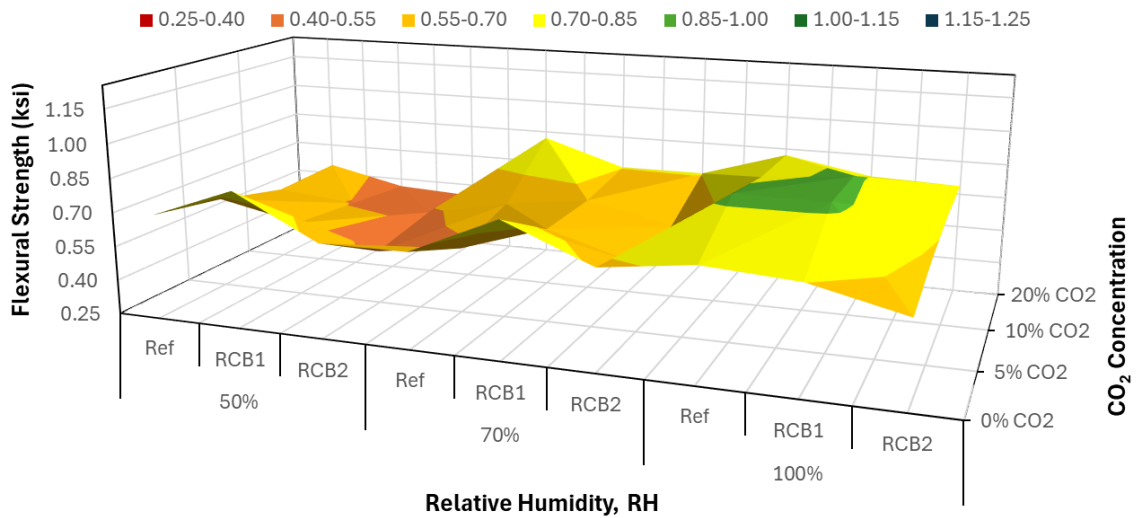


Figure 28. 3- Day Flexural Strength of Mortars Cured in Varying CO<sub>2</sub> Concentrations and Relative Humidities

Surface plots from compressive strength testing show that increasing CO<sub>2</sub> and humidity result in optimal strengths (Figure 29). For all mix types, the highest strengths are achieved with 20% CO<sub>2</sub> and 100% RH. Decreasing humidity, high CO<sub>2</sub> concentrations can be detrimental to compressive strength.

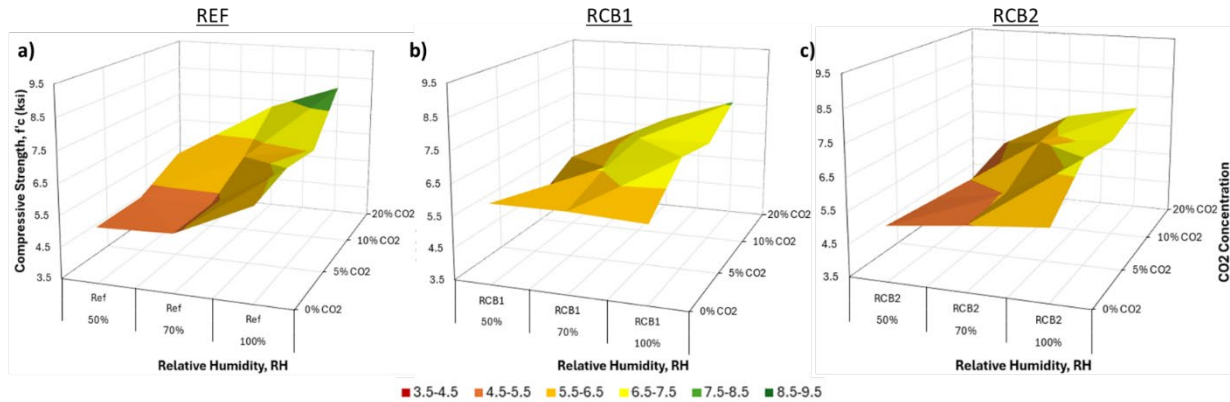


Figure 29. 3- Day  $f'_c$  of Ref. (a), RCB1 (b), and RCB2 (c) Mortars Cured in Varying CO<sub>2</sub> Concentrations and Relative Humidities

### 5.9. Effects of different CO<sub>2</sub> curing conditions, temperature and humidity on the carbonation depth of mortars

Phenolphthalein images in Figure 30 display the cross-sections of CO<sub>2</sub>-cured samples treated with phenolphthalein. While there remains little difference between cross-sectional pH in nanomodified and reference mix groups, these images show differences in the carbonation depth depending on the RH during the CO<sub>2</sub> exposure; the higher the RH, the lower the carbonation depth. For 50% RH samples, increasing CO<sub>2</sub> concentrations from 5% to 20% nearly doubles the carbonation depth of all mixed types. For 70% RH samples, the same increase in CO<sub>2</sub> increases carbonation depth from approximately 0.1" to 0.15" (just 50%). When evaluating 20% CO<sub>2</sub> treated samples, carbonation depth is reduced by approximately 0.15", from 0.3" to almost zero, between 50% and 100% RH. These carbonation patterns imply that at lower humidities, the CO<sub>2</sub> curing induces a reduction of the pH and CO<sub>2</sub> penetrates deeper into mortar specimens, while at 100% RH, different modes of carbonation may occur that do not reduce pH, nor do they interfere with hydration development.

Upon evaluating the results of flexural and compressive testing, it was determined that the optimal curing conditions for future samples during the comparison cure phase are 20% CO<sub>2</sub> at 100% RH. These conditions result in the highest compressive strength for all mix types and provide strengths comparable to or higher than steam curing (Figure 29) without affecting the carbonation depth in comparison with non-CO<sub>2</sub> cured samples (Figure 23), potentially functioning as a more energy-efficient alternative to heat curing used in the precast industry with no effects on corrosion. For all subsequent tasks, samples cured in this condition are identified as "CO<sub>2</sub>-cured".

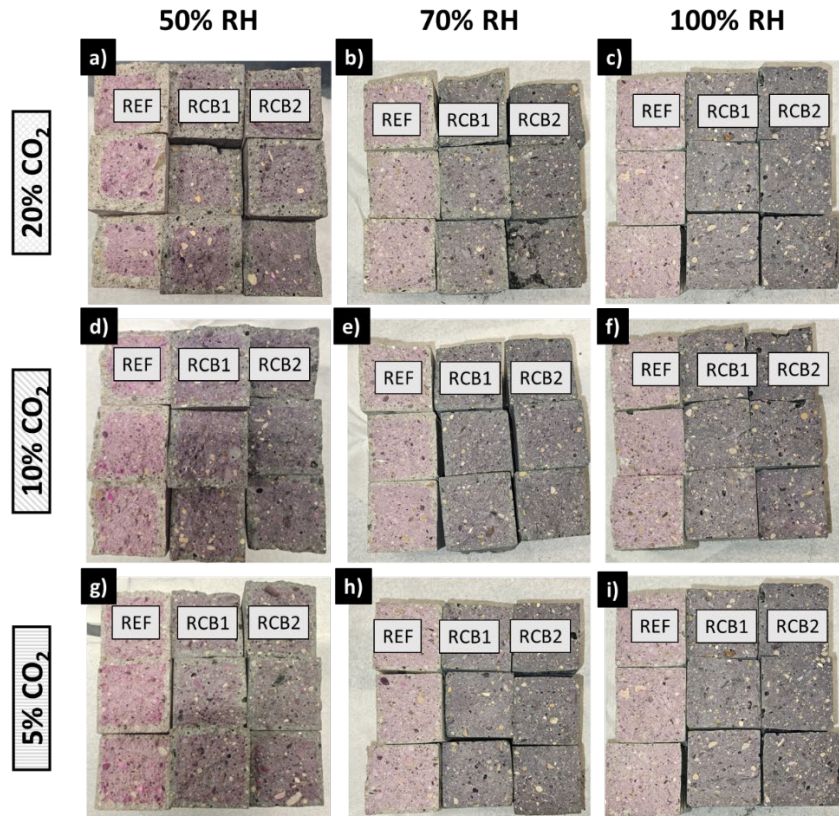


Figure 30. Phenolphthalein Treated Cross-Sections of Mortar Cured in Varying  $CO_2$  at  $23^\circ C$

### 5.10. Corrosion Testing

#### Casting and preparation of corrosion test samples.

No. 4 steel rebar was prepared according to ASTM G109. After cleaning the rebar free of rust, 2.5" of the top and 0.75" of the bottom portions were wrapped in electroplaters tape, covered in two-part epoxy, wrapped in heat-shrink polyolefin tube, and ends sealed with electroplaters tape, leaving approximately 2" of rebar exposed (Figure 31). 2" by 4" mortar cylinders were cast and the prepared rebar inserted in the center of each sample while the mortar was fresh (Figure 31).



Figure 31. Preparation of Rebar for Lollipop Corrosion Sample

After curing in molds for 16 hours, samples were split into two groups: wet cured samples cured in 100% RH and 23°C, and CO<sub>2</sub> cured samples cured in 100% RH, 20% CO<sub>2</sub>, and 23°C. These samples were cured according to the curing regimen described in Task 2 and subsequently cured until 28 days of hydration in 50%RH at 23°C. After 28 days of hydration, samples were immersed in 3.5" of 16.5% NaCl solution in glass jars, surrounded by steel mesh tubing to await corrosion potential ( $E_{corr}$ ), corrosion current ( $I_{corr}$ ), and current density evaluation.

### Corrosion testing and results

A Zahner IM6 Electrical Impedance Measurement Unit will be used for all electrochemical assessments in this study. The open-circuit potential ( $E_{ocp}$ ) difference between the silver chloride reference electrode (RE) and steel rebar working electrode (WE) in each sample will be measured and recorded. After ensuring the  $E_{ocp}$  remained stable over a 1 minute period, polarization scans will begin over range of -30mV to 30mV.

Specimens are currently saturating in NaCl solution (Figure 32) for a minimum of 7 days to avoid having to account for a potential ohmic drop during readings. Initial testing was attempted on some of the samples, but the steel mesh counter electrodes began to rust the next day, possibly due to hyperpolarization of the counter electrode during testing. To avoid damaging any additional test specimens, new polarization parameters will be researched during the week of submission of this document to use for future testing instead. The corrosion results from this test will be acquired by the end of this project (End of December 2026).



Figure 32. Lollipop Corrosion Specimens Submerged in 16.5% NaCl Solution

### 5.11. Effect of nano-additives and CO<sub>2</sub> curing on the wettability of cementitious composites.

The smooth, bottom face of each cylinder was used for wettability analysis per ASTM D7334<sup>34</sup>. A 15  $\mu$ L syringe was used to dispense 3 droplets of distilled water onto the smooth, even faces of each cylinder (Figure 33). The application of each droplet was recorded via digital video over a span of 10 seconds. Using MATLAB and image analysis tools, the angles of contact between the droplets and the sample surfaces were measured at 0, 1, 5, and 10 seconds after contact. At each time interval, the contact angles for each droplet were averaged to determine the degree of wettability for each mix and curing type, and to determine the rate at which the droplet is absorbed into the sample surface. Contact angles less than 45° indicate a hydrophilic surface, while contact angles more than 90° indicate a hydrophobic surface.

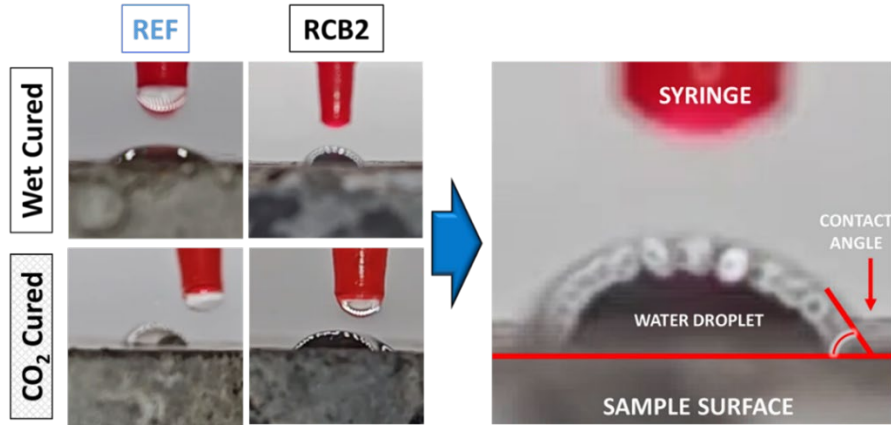


Figure 33. Water Droplet on REF and RCB2 Mortar Cylinders at Initial Point of Contact

Figure 34 summarizes the results of the wettability test with 2% RCB versus no RCB (reference) for both wet-cured and CO<sub>2</sub>-cured samples. Results show that 2% RCB reduces the hydrophilic behavior of the cementitious composites. Furthermore, while, for reference, CO<sub>2</sub> curing reduces hydrophilic behavior, perhaps due to a reduction in surface porosity, for the material with 2% RCB, CO<sub>2</sub> curing does not affect wettability.

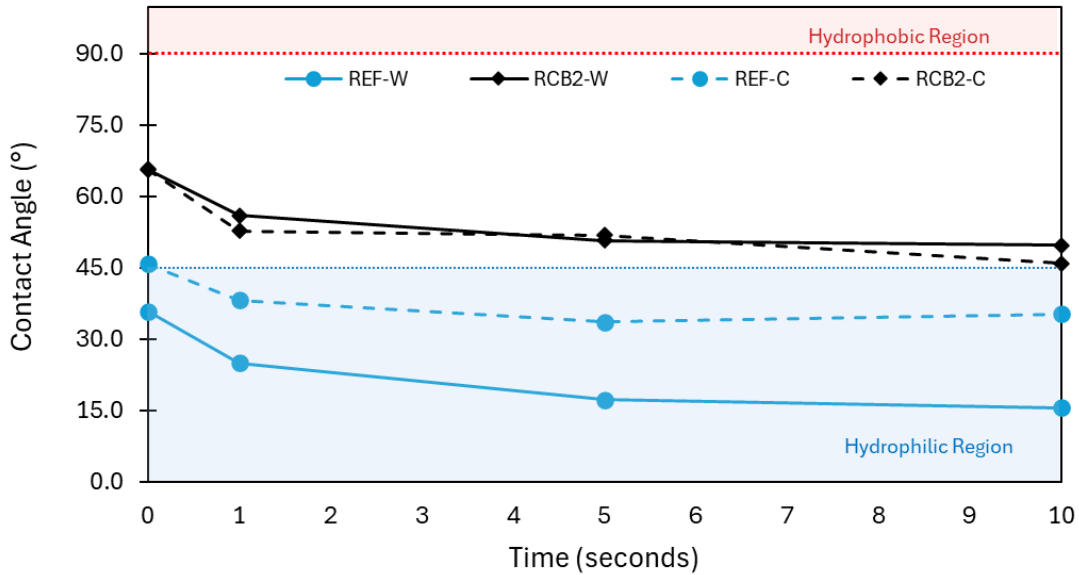


Figure 34. Contact Angle of Droplets on REF vs RCB2 Mortar Cylinders Over Time with and without CO<sub>2</sub> curing

## 6. Outreach activities related to the project.

Various outreach activities have been completed throughout the duration of the project, facilitating collaboration among high school, collegiate, and industrial parties. These activities can be separated into 2 categories: educational outreach and workforce development.

### Educational Outreach

Minority in Engineering Program's "Purdue Promise": Minority in Engineering Program's "Purdue Promise": Civil Engineering Tours. Purdue University West Lafayette, Indiana. October 13<sup>th</sup>, 2024. (Fig. 35)

Purdue University's Minority in Engineering Program hosts "Purdue Promise" annually to encourage high school applications and enrollment to Purdue University engineering schools.

On October 13<sup>th</sup>, 2024, the graduate student on this project and other members of the Lyles School of Civil and Construction Engineering hosted a tour for visiting high schoolers to give them a preview of the innovative engineering technologies. What was expected to be a group of 10 turned into 22 high school tourists by request. This project was featured with many others as a talking point for the tours.

Civil Engineering (CE) Experience correspondence: Civil Engineering Experience: Merrillville High School Merrillville, Indiana; December 2024. <https://mhsmirrornews.com/3597/showcase/mhs-grad-introduces-students-to-wonders-of-engineering-2/>

A STEM education event hosted by the graduate student on December 12<sup>th</sup>, of 2024. Though it was initially planned to showcase engineering demonstrations and lessons to around 50 highschoolers, the event quickly gained traction, and hundreds of students attended the event throughout the day. The event was comprised of 4 demonstration sessions covering structural engineering, college planning, hydraulics engineering, and materials engineering, which featured the nanomaterials used in this project.

Office of Undergraduate Research (OUR) Scholars: Three undergraduate 3rd-year Purdue students, all from minority or underrepresented groups, have earned university credit through this project, two of which have received scholarships through the OUR scholarship program at Purdue. For this program, students participate in research experiments, analysis, and create reports and



Figure 35. Highschool students that attended Purdue Promise 2024, almost half of which participated in the lab tours supported by this project (Courtesy of the Minority in Engineering Program, Purdue University)



Figure 36. Aniya Edwards (graduate student on this project), hosting the CE Experience to highschoolers at Merrillville Highschool, Merrillville, IN

presentations for their end of the year research symposium. At the end of the spring semester, one of the students began an internship in the civil engineering industry, while another continued their studies and received multiple awards for their involvement in the civil engineering program.

Aniya Edwards Master's Thesis Defense:  
*Thesis Defense Presentation – A.Edwards.*  
*“Enhancing Cementitious Composites Through Waste Valorization: The Effect of Multiscale Recycled Materials on the Properties of Mortars”.*  
*Purdue University Graduate School.*  
<https://doi.org/10.25394/PGS.28899938.v1>

Select results from this project were presented in the graduate student's public master's thesis defense, where several graduate and undergraduate students attended to learn more about civil engineering research at Purdue University. Aniya Edwards passed her defense and received her master's degree in the Spring of 2025 (Figure 37). She began the PhD program at Purdue University in the Summer of 2025. The thesis will be made available to the public in 2027.



Figure 37. From left to right: Dr. Raikhan Tokpatayeva (virtual meeting), Professor Mirian Velay-Lizancos, Aniya Edwards, Professor Antonio Bobet, Professor Jan Olek after the Aniya Edwards' master's thesis defense

### Workforce Development

Our team has had the opportunity to participate in several workforce development events through this project. A variety of presentations were given at these events, which provided clarity to industrial professionals interested in sustainable concrete practices. Examples:

TRANS-IPIC UTC 2024 Spring Workshop: 2024  
Trans-IPIC UTC Workshop. 2024 TRANS-IPIC UTC  
Workshop. <https://trans-ipic.illinois.edu/workshop>  
(Fig. 38).



Figure 38. Research presentation by Aniya Edwards, presenting the project results at TRANS-IPIC UTC Spring Workshop 2025, Rosemont, IL.

Future of Transportation Summit : United Stated  
Department of Transportation Future of Transportation Summit – August 13<sup>th</sup>, 2024. List of  
Posters. FoT Summit. (n.d.). [https://fot-summit.org/?page\\_id=692](https://fot-summit.org/?page_id=692) (Fig. 39).

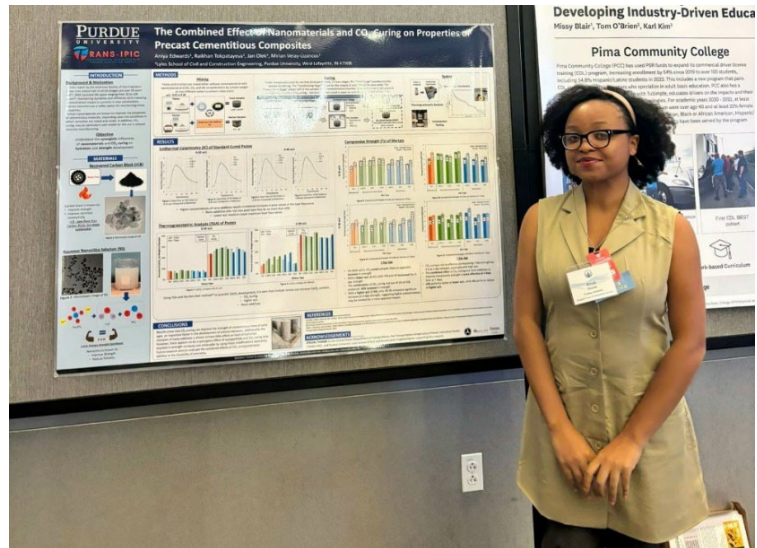


Figure 39. Poster presentation by the graduate student Aniya Edwards presenting the project results at the Future of Transportation Summit hosted by the USDOT at their headquarters in Washington D.C. in August 2024.

TRANS-IPIC UTC Monthly Research Webinars:

A fifteen-minute presentation was prepared and presented for the monthly research webinar hosted by TRANS-IPIC on June 17<sup>th</sup>, 2024 and August 22<sup>nd</sup>, 2025. This presentation was made available to the public.

- Trans-IPIC Monthly Research Webinar - June, 2024. Illinois Media Space. (n.d.). [https://mediaspace.illinois.edu/media/t/1\\_xt7op9zl](https://mediaspace.illinois.edu/media/t/1_xt7op9zl)
- Trans-IPIC Monthly Research Webinar – Aug., 2025. Illinois Media Space. (n.d.). <https://trans-ipic.illinois.edu/August-2025-Webinar>

C3 Symposium: Extended abstract and Oral Presentation - A. Edwards, R. Tokpatayeva, J. Olek, and M. Velay-Lizancos, “Synergistic Effects of CO2 Curing and Recovered Carbon Black Nano additives on Early Age Performance of Cementitious Composites”: C3 Symposium 2025. Chicago, IL. 10/02-05/2025. <https://carbonconcrete.com/#key-dates-4095>. (Fig. 40).



Figure 40. Oral presentation by the graduate student Aniya Edwards presenting the project results at the C3 Symposium in Chicago, IL in October 2025

### Precast Concrete Facility Tours and Talks:

The graduate student facilitated the correspondence between several precast concrete manufacturers in the Midwest. A plant tour (hosted by TransIPIC at the 2025 TransIPIC Spring Workshop) and subsequent web meeting with Dukane Precast in Naperville, IL, as well as a plant tour and meeting with County Materials in Maxwell, IN (Figure 41) helped in mixture selection and planning during this project. During these meetings the students interviewed different members of both companies on precast concrete curing procedures, manufacturing obstacles, logistics, and priorities for the different industrial sectors they serve.



*Figure 41. Graduate student Aniya Edwards during plant tour County Materials in Maxwell, IN*

## 7. Conclusions and recommendations

To be used as an additive, recovered carbon black requires a special dispersion method to avoid agglomeration. Mixing the RCB with a small amount of water using a high-shear mixer-blender significantly reduces agglomeration compared to the dry mix method.

Notable differences were found between the composition and mechanical characterization of CO<sub>2</sub>-cured and standard-cured cementitious specimens with and without nano-additives (nano-silica and recovered carbon black) at two different water-to-cement (w/c) ratios. Thermogravimetric analysis shows that CO<sub>2</sub> curing greatly improved the CaCO<sub>3</sub> content in samples compared to standard curing. The incorporation of nanoadditives is shown to increase the CaCO<sub>3</sub> content in higher w/c samples, especially when used with CO<sub>2</sub> curing. Compressive test results showed a strength increase in CO<sub>2</sub>-cured specimens compared to standard-cured specimens. Results indicated that the combination of CO<sub>2</sub> curing and nano-additive use resulted in the highest early compressive strength among all mixtures and curing conditions studied (which is very important for precast production), while reducing the calcium hydroxide content, thus potentially reducing the risk of durability issues such as calcium oxychloride formation.

The combination of nanoparticles addition and 12-hour 50°C CO<sub>2</sub> curing process can provide comparable strength to non-nanomodified concretes with a 24-hour 50°C wet curing; reducing the time of high curing temperatures required to achieve the target early strength.

Furthermore, it was observed that 20% CO<sub>2</sub> curing (no heating) samples achieved comparable or superior strength than the 50 °C curing option, for reference and 1% RCB, suggesting that CO<sub>2</sub> curing without heating can be an alternative to steam curing in terms of accelerating the early strength development required to maximize the production of precast elements.

Furthermore, the optimal CO<sub>2</sub> concentration to enhance early strength depends strongly on the relative humidity during exposure. Besides, the effectiveness of RCB and CO<sub>2</sub> curing highly depends on the relative humidity. Still, across all mixes, the highest strengths are achieved with 20% CO<sub>2</sub> and 100% RH, without affecting carbonation depth relative to non-CO<sub>2</sub>-cured samples, potentially serving as a more energy-efficient alternative to heat curing used in the precast industry, with no effects on corrosion. Additionally, the CO<sub>2</sub>-curing method reduces the porosity of both the reference and RCB samples.

For non-nanomodified mixes, CO<sub>2</sub> curing reduces the hydrophilicity of the cementitious composite, potentially due to a reduction in surface porosity produced during CO<sub>2</sub> curing. The use of 2% RCB clearly increases the hydrophobicity of the composite, but CO<sub>2</sub> curing does not produce a further increase.

## 8. Practical application/impact on transportation infrastructure

Many precast companies use heating during the curing process to accelerate early strength development and increase production volume without sacrificing durability, as early removal of the forms or transportation of elements with insufficient strength can lead to macro-cracking or micro-cracking.

This project has demonstrated that it is possible to reduce the curing time at high temperatures by half by combining CO<sub>2</sub> curing with the addition of recovered carbon black. Thus, this approach can reduce energy consumption and increase precast production, potentially reducing the cost of precast infrastructure elements. Furthermore, when optimized, CO<sub>2</sub> curing not only reduces the time to achieve the target early strength but also reduces porosity, a critical factor in enhancing durability.

While this project, with Phases I and II, helped pave the way for the optimized utilization of CO<sub>2</sub> curing methods in the precast industry to produce more durable precast elements at a faster rate, further steps are required for full implementation of these advancements. The implementation of the optimized curing method requires developing and implementing a CO<sub>2</sub> curing system adapted to the different precast elements. A partnership with a precast company is required to develop and implement a prototype, and the optimization of the curing process may also be dependent on the mixture design used by the precast company.

## 9. References

1. C. Moro, V. Francioso, M. Schager, M. Velay-Lizancos, M. Schragger, M. Velay-Lizancos, TiO<sub>2</sub> nanoparticles influence on the environmental performance of natural and recycled mortars: A life cycle assessment, *Environ. Impact Assess. Rev.* 84 (2020) 106430.
2. D. Bonen, M.D. Cohen, Magnesium sulfate attack on portland cement paste-I. Microstructural analysis, *Cem. Concr. Res.* 22 (1992) 169–180. [https://doi.org/10.1016/0008-8846\(92\)90147-N](https://doi.org/10.1016/0008-8846(92)90147-N).
3. D. Bonen, M.D. Cohen, Magnesium sulfate attack on portland cement paste — II. Chemical and mineralogical analyses, *Cem. Concr. Res.* 22 (1992) 707–718. [https://doi.org/10.1016/0008-8846\(92\)90023-O](https://doi.org/10.1016/0008-8846(92)90023-O).
4. M. Santhanam, M.D. Cohen, J. Olek, Mechanism of sulfate attack: A fresh look: Part 1: Summary of experimental results, *Cem. Concr. Res.* 32 (2002) 915–921. [https://doi.org/10.1016/S0008-8846\(02\)00724-X](https://doi.org/10.1016/S0008-8846(02)00724-X).
5. P. Suraneni, J. Monical, E. Unal, Y. Farnam, J. Weiss, Calcium oxychloride formation potential in cementitious pastes exposed to blends of deicing salt, *ACI Mater. J.* 114 (2017) 631–641. <https://doi.org/10.14359/51689607>.
6. C. Jones, S. Ramanathan, P. Suraneni, W.M. Hale, Calcium oxychloride: A critical review of the literature surrounding the formation, deterioration, testing procedures, and recommended mitigation techniques, *Cem. Concr. Compos.* 113 (2020). <https://doi.org/10.1016/J.CEMCONCOMP.2020.103663>.
7. S. Chatterji, The role of Ca(OH)<sub>2</sub> in the breakdown of Portland cement concrete due to alkali-silica reaction, *Cem. Concr. Res.* 9 (1979) 185–188. [https://doi.org/10.1016/0008-8846\(79\)90024-3](https://doi.org/10.1016/0008-8846(79)90024-3).
8. T. Kim, J. Olek, H.G. Jeong, Alkali-silica reaction: Kinetics of chemistry of pore solution and calcium hydroxide content in cementitious system, *Cem. Concr. Res.* 71 (2015) 36–45. <https://doi.org/10.1016/J.CEMCONRES.2015.01.017>.
9. C. Carde, R. François, Effect of the leaching of calcium hydroxide from cement paste on mechanical and physical properties, *Cem. Concr. Res.* 27 (1997) 539–550. [https://doi.org/10.1016/S0008-8846\(97\)00042-2](https://doi.org/10.1016/S0008-8846(97)00042-2).

10. Chen, T., and Gao, X.: Use of carbonation curing to improve mechanical strength and durability of Pervious Concrete." ACS Sustainable Chemistry & Engineering, vol. 8, no. 9, 20 pp. 3872–3884(2020)
11. Moro, C., Francioso, V., Velay-Lizancos, M.: Impact of nano-TiO<sub>2</sub> addition on the reduction of net CO<sub>2</sub> emissions of cement pastes after CO<sub>2</sub> curing. Cement and Concrete Composites, 123 (2021) 104160.
12. "ASTM C642-21 ." ASTM C642-21 Standard Test Method for Density, Absorption, and Voids in Hardened Concrete, ASTM Int., 2021, compass.astm.org/content-access?contentCode=ASTM%7CC0642-21%7Cen-US.
13. ASTM. C1585-20 Standard Test Method for Measurement of Rate of Absorption of Water by Hydraulic Cement Concretes. *ASTM Int.* Published online 2020:1-6. doi:10.1520/C1585-20.2
14. ASTM C1876 Standard test method for bulk electrical resistivity or bulk conductivity of concrete. (2024). *ASTM Int.* <https://doi.org/10.1520/c1876>
15. ASTM C1202-25. ASTM C1202-25 Standard Test Method for Electrical Indication of Concrete's Ability to Resist Chloride Ion Penetration, ASTM International, 2025, compass.astm.org/content-access?contentCode=ASTM%7CC1202-25%7Cen-US.
16. ASTM. C39/39M-21 Standard Test Method for Compressive Strength of Cylindrical Concrete Specimens. ASTM Int. Published online 2021:1-5. doi:10.1520/C0039
17. ASTM Int. "ASTM G109-23." ASTM G109-23 Standard Test Methods for Determining Effects of Chemical Admixtures on Corrosion of Embedded Steel Reinforcement in Concrete Exposed to Chloride Environments, 2023, compass.astm.org/content-access?contentCode=ASTM%7CG0109-23%7Cen-US.
18. Ariyachandra, Erandi, et al. "Effect of NO<sub>2</sub> sequestered recycled concrete aggregate (NRCA) on mechanical and durability performance of concrete." Cement and Concrete Research, vol. 137, Nov. 2020, p. 106210, <https://doi.org/10.1016/j.cemconres.2020.106210>.
19. Mishra, Shubham, et al. "Mechanistic evaluation of NO<sub>2</sub> sequestered recycled concrete aggregates as anodic corrosion inhibitors in chloride-exposed OPC Concrete: Insights from kinetics and performance assessment." Materials and Structures, vol. 58, no. 4, 16 Apr. 2025, <https://doi.org/10.1617/s11527-025-02625-w>.
20. ASTM Int. "ASTM C876-22b." ASTM C876-22b Standard Test Method for Corrosion Potentials of Uncoated Reinforcing Steel in Concrete, 2022, compass.astm.org/content-access?contentCode=ASTM%7CC0876-22B%7Cen-US.
21. ASTM C136 Standard test method for sieve analysis of fine and coarse aggregates. ASTM Int. Accessed December 30, 2023. <https://www.astm.org/standards/c136>.
22. Sieve analysis of fine and coarse aggregates AASHTO T 27 - in.gov. Accessed December 30, 2023. [https://www.in.gov/indot/div/mt/aashto/testmethods/aashto\\_t27.pdf](https://www.in.gov/indot/div/mt/aashto/testmethods/aashto_t27.pdf).
23. ASTM C127 Standard test method for relative density (specific gravity) and absorption of coarse aggregate. *ASTM Int.* Accessed December 30, 2023. <https://www.astm.org/standards/c127>.
24. ASTM C128-22 Standard Test Method for Relative Density (Specific Gravity) and Absorption of Fine Aggregate. *ASTM Int.* Accessed February 29, 2024.

25. ASTM C305-20 Standard Practice for Mechanical Mixing of Hydraulic Cement Pastes and Mortars of Plastic Consistency. *ASTM Int.* Accessed March 31, 2024. <https://compass.astm.org/document/?contentCode=ASTM%7CC0305-20%7Cen-US>
26. ASTM C192/C192M-19 Standard Practice for Making and Curing Concrete Test Specimens in the Laboratory. *ASTM Int.* Accessed September 30, 2024. [https://compass.astm.org/document/?contentCode=ASTM%7CC0192\\_C0192M-19%7Cen-US](https://compass.astm.org/document/?contentCode=ASTM%7CC0192_C0192M-19%7Cen-US)
27. ASTM. C642-21 Standard Test Method for Density, Absorption, and Voids in Hardened Concrete. *ASTM Int.* Published online 2021:1-3. doi:10.1520/C0642-21.2
28. ASTM. C1585-20 Standard Test Method for Measurement of Rate of Absorption of Water by Hydraulic Cement Concretes. *ASTM Int.* Published online 2020:1-6. doi:10.1520/C1585-20.2
29. T. Kim, J. Olek, "Effects of Sample Preparation and Interpretation of Thermogravimetric Curves on Calcium Hydroxide in Hydrated Pastes and Mortars", *Transp. Res. Rec. J. Transp. Res. Board*, 10-18, 2290 (2012).
30. "NPCA Quality Control Manual For Precast Concrete Plan." NPCA Quality Control Manual For Precast Concrete Plan, National Precast Concrete Association (NPCA), 1 Feb. 2024, [precast.org/wp-content/uploads/020124\\_QualityControlManual\\_17th\\_Edition.pdf](http://precast.org/wp-content/uploads/020124_QualityControlManual_17th_Edition.pdf).
31. "ASTM C348-21." ASTM C348-21 Standard Test Method for Flexural Strength of Hydraulic-Cement Mortars, ASTM Int., 2021, [compass.astm.org/content-access?contentCode=ASTM%7CC0348-21%7Cen-US](https://compass.astm.org/content-access?contentCode=ASTM%7CC0348-21%7Cen-US).
32. ASTM. ASTM C349-24 Standard Test Method for Compressive Strength of Hydraulic-Cement Mortars (Using Portions of Prisms Broken in Flexure), ASTM Int., 2024, [www.astm.org/c0349-18.html](http://www.astm.org/c0349-18.html).
33. Songolzadeh, Mohammad, et al. "Carbon Dioxide Separation from Flue Gases: A Technological Review Emphasizing Reduction in Greenhouse Gas Emissions." *TheScientificWorldJournal*, U.S. National Library of Medicine, 17 Feb. 2014, [pmc.ncbi.nlm.nih.gov/articles/PMC3947793/](http://pmc.ncbi.nlm.nih.gov/articles/PMC3947793/).
34. "ASTM D7334-08(2022)." ASTM D7334-08(2022) Standard Practice for Surface Wettability of Coatings, Substrates and Pigments by Advancing Contact Angle Measurement, ASTM Int., 2022, [compass.astm.org/content-access?contentCode=ASTM%7CD7334-08R22%7Cen-US](https://compass.astm.org/content-access?contentCode=ASTM%7CD7334-08R22%7Cen-US).